NOVEL MONOMERIC AND POLYMERIC PHOTOINITIATORS WITH TYPE II AND (TYPE I-OR-H-DONOR) SIDE CHAINS

by

Fulya Köylü

B.S., Chemistry, Boğaziçi Üniversitesi, 2011

Submitted to the Institute for Graduate Studies in
Science and Engineering in partial fulfillment of
the requirements for the degree of
Master of Science

Graduate Program in Chemistry
Boğaziçi University
2015

Dedicated to my supporting family and friends...

ACKNOWLEDGEMENTS

First of all, I would like to deeply thank my supervisor Prof. Duygu Avcı Semiz for her systematic guidance and her encouragement that made it possible for me to complete this study. I gained a great deal of experience thanks to her endless support and attention.

I would like to extend my appreciation to my committee members Prof. Turgut Nugay and Prof. Ayşen Önen for generously giving their valuable time for reviewing the final manuscript and for their constructive comments and suggestions.

I would also like to thank all members of the Chemistry Department who were always eager to help me throughout my whole chemistry experience.

My deepest gratitude goes to Sesil Agopcan Çınar and Tuğçe Nur Eren for their grand help and guidance during my time in the laboratory. I also thank my dear group friends Belgin Cesur, Betül Bingöl, Melek Naz Güven and Ece Akyol for their help and supportive friendship.

I also wish to thank my dear friends Begüm Pekmezci, Cansu Gürler, Onur Gündüz and Thomas Arnold for their endless support since the day I met them.

Finally, my greatest gratitude is extended to my family members for their endless love, support and understanding. My mother deserves an extended appreciation for her continuous encouragement in everything I do in my life.

This research was supported by The Scientific and Technological Research Council of Turkey (TÜBİTAK) [113Z241] and Bogazici University Research Fund (9700).

ABSTRACT

NOVEL MONOMERIC AND POLYMERIC PHOTOINITIATORS WITH TYPE II AND (TYPE I-OR-H-DONOR) SIDE CHAINS

A recent trend in the effort to develop high performance photoinitiator (PI) systems for photopolymerization is to consider polymerizable or polymeric ones. These have some advantages such as high reactivity, low volatility and low migration in comparison with low-molecular weight nonmonomeric analogues. In this work, methacrylate monomers containing both Type I (Irgacure 2959) and Type II (benzophenone or thioxanthone) groups (PI1 and PI3) and both PI (benzophenone) and a coinitiator (sesamol) (PI2) in their structures were successfully synthesized. The copolymerizations of these monomeric photoinitiators with butyl methacrylate [PPI (BMA-*co*-PI1), PPI (BMA-*co*-PI2) and PPI (BMA-*co*-PI3)] were carried out to investigate the properties of polymeric photoinitiators. The photopolymerization efficiencies of the synthesized photoinitiators were investigated in the polymerizations of 1,6-hexanedioldiacrylate by real-time Fourier transformation infrared spectroscopy (FTIR) and compared with small molecule photoinitiators they are synthesized from (benzophenone, thioxanthone and Irgacure 2959). Broadband irradiation experiments for excitation of both chromophoric groups of PI1 and PI3 indicated no improvement on the efficiencies compared to their physical mixtures (BP/Irgacure 2959 and TX/Irgacure 2959). PI2-based one component PI systems were found to be an alternative to the use of conventional amine coinitiators.

ÖZET

TİP II VE (TİP I YA DA H-VERİCİ) YAN ZİNCİRLERE SAHİP YENİ MONOMERİK VE POLİMERİK FOTOBAŞLATICILAR

Fotopolimerizasyonda kullanılacak yüksek performanslı fotobaşlatıcı sistemlerini geliştirme çalışmalarında yakın zamanlardaki eğilim polimerize olabilen veya polimerik fotobaşlatıcıları göz önünde bulundurmaktır. Düşük moleküler ağırlıklı monomer olmayan analogları ile karşılaştırıldıkları zaman bu fotobaşlatıcıların bazı avantajlara sahip oldukları belirlenmiştir. Örnek olarak, yüksek reaktivite, düşük uçuculuk ve düşük migrasyon gösterilebilir. Bu çalışmada hem tip I (Irgacure 2959) hem de tip II (benzofenon yada tiyokzanton) (PI1 ve PI3) ve hem fotobaşlatıcı (benzofenon) hem de hidrojen donör (sesamol) (PI2) gruplarını içeren metakrilat monomerleri başarıyla sentezlenmiştir. Polimerik fotobaşlatıcıların özelliklerini araştırabilmek için sentezlenen monomerik fotobaşlatıcıların bütil metakrilat ile kopolimerleri [PPI (BMA-*co*-PI1), PPI (BMA-*co*-PI2) and PPI (BMA-*co*-PI3)] üretilmiştir. Sentezlenen fotobaşlatıcıların fotopolimerizasyon verimliliklerini araştırmak için 1,6-hekzandioldiakrilatı fotopolimerleştirme etkinlikleri gerçek-zamanlı Fourier dönüşümü kızılötesi tayfölçümü (FTIR) aracılığıyla incelenmiştir ve sonuçlar düşük moleküler ağırlıktaki fotobaşlatıcılarla (benzofenon, tiyokzanton ve Irgacure 2959) karşılaştırılmıştır. Hem PI1 hem PI3'ün kromoforik gruplarının uyarılması amacıyla yapılan geniş bantlı ışınlama deney sonuçları karşılaştırıldıkları fiziksel karışımlara (BP/Irgacure 2959 ve TX/Irgacure 2959) göre bir gelişme göstermemişlerdir. PI2 bazlı tek bileşenli PI sistemleri geleneksel amin eşbaşlatıcılar yerine bir alternatif olarak uygun bulunmuştur.

TABLE OF CONTENTS

LIST OF TABLES

LIST OF FIGURES

LIST OF SYMBOLS

E_T	Triplet state energy
[I]	Concentration of the initiator
I_a	Intensity of absorbed light
k_p	The rate constant of the propagation reaction
k_t	The rate constant of the termination reaction
[M]	Concentration of the monomer
M_n	The number average molecular weight
PDI	Polydispersity index
PI	Photoinitiator
PPI	Polymeric photoinitiator
PI1	4-benzoylphenyl2-((2-(4-(2-hydroxy-2-methylpropanoyl) phenoxy)ethoxy)methyl)acrylate
PI2	Benzo[d][1,3]dioxol-5-yl 2-((4-benzoylphenoxy)methyl) acrylate
PI3	2-(4-(2-hydroxy-2-methylpropanoyl)phenoxy)ethyl 2-(((9-oxo-9*H*-thioxanthen-2-yl)oxy)methyl)acrylate
PS	Photosensitizer
Q / s	Heat flow per second
R_i	Rate of initiation
R_{pmax}	The maximum rate of polymerization
R_p	Rate of polymerization
t_{max}	Time to the maximum polymerization rate

ΔH_p	Heat released per mole of double bonds reacted
ε	Extinction coefficient
λ_{max}	The wavelengths for maximum absorption

LIST OF ACRONYMS / ABBREVIATIONS

AIBN	2,2'-Azobisisobutyronitrile
AQ	Anthraquinone
BMA	Butyl methacrylate
BP	Benzophenone
CQ	Camphorquinone
CW	Continuous wave
DABCO	1,4-Diazabicyclo[2.2.2]octane
DCM	Dichloromethane
DMAEM	N,N-dimethylaminoethyl methacrylate
DMF	Dimethylformamide
DMPA	2,2-dimethoxy-2-phenyl-aetophenone
DMSO	Dimethyl sulfoxide
DPC	Differential Photocalorimeter
DSC	Differential Scanning Calorimetry
EDAB	Ethyl 4-dimethylaminobenzoate
FT-IR	Fourier Transform Infrared Spectroscopy
GPC	Gel Permeation Chromatography
HAP	2-hydroxy-2-methyl-1-phenyl-1-propanone
HCAP	1-hydroxy-cyclohexyl-1-phenyl ketone
HDDA	Hexane-1,6-diol diacrylate

HEA	Hydroxyethyl Acrylate
IRGACURE 2959	2-Hydroxy-1-[4-(2-hydroxyethoxy)phenyl]-2-methyl-1-propanone
MMA	Methyl methacrylate
MPPK	2-Benzyl-2-dimethylamino-1-(4-morpholinophenyl)-1-butanone
NMR	Nuclear Magnetic Resonance spectroscopy
PEG	Polyethylene glycol
TBBr	*Tert*-butyl α–bromomethacrylate
TBBr-BP	*Tert*-butyl 2-((4-benzoylphenoxy)methyl)acrylate
TBBr-BP-CA	2-((2-(4-(2-hydroxy-2-methylpropanoyl)phenoxy)ethoxy) methyl) acrylic acid
TBBr-TX	*tert*-butyl 2-((9-oxo-9H-thioxanthen-2-yloxy)methyl)acrylate
TBBr-TX-CA	2-((9-oxo-9H-thioxanthen-2-yloxy)methyl)acrylic acid
TBHMA	*Tert*-butyl α–hydroxymethacrylate
T_g	Glass transition temperature
TGA	Thermal Gravimetric Analysis
THF	Tetrahydrofuran
TMPTA	Trimethylolpropane triacrylate
TPMK	2-methyl-1-(4-methylthiobenzoyl)-2-morpholino-propan-1-one
TX	Thioxanthone

1. INTRODUCTION: PHOTOPOLYMERIZATION

Photopolymerization is a field that is recognized widely for its economic and ecological advantages in industrial applications including coatings, inks, adhesives, electronics and dental fillings [1-3]. Photopolymerization is preferred over thermal polymerization which usually requires high temperatures, whereas photopolymerization can be performed at room temperature or below [3]. Photopolymerization is considered a green technology due to low temperature operation and less VOC emissions as a result of solvent-free formulations [4-5]. Also, because of the fact that light is easily controlled in space, curing can be carried out in specific areas, which is quite beneficial in the production of electronic devices. Moreover, photopolymerization comes with the advantage of easy handling and avoidance of loss of material as a result of premature gelation, because the possibility of "cure on demand" triggered by light gives full control over the curing process.

Photopolymerization is a chain process that is initiated by light and where the initiating species and the growing chain ends are radicals or cations (Figure 1.1). The initiating species are called photoinitiators and they are activated by light. Following their activation they attack the monomers or oligomers to form linear or crosslinked polymers [6].

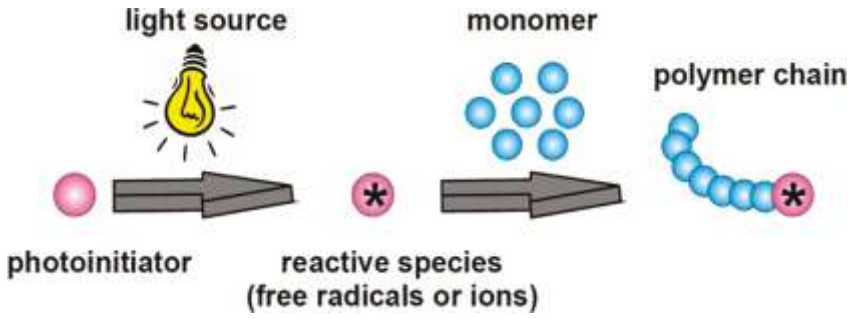

Figure 1.1. Photopolymerization process [3].

1.1. Photoinitiated Free-Radical Polymerization

Photoinitiated free-radical polymerization has attracted quite an interest due to being applicable to a wide variety of acrylate-based resins [7]. Radical polymerization includes four steps; photoinitiation, propagation, chain transfer and termination (Figure 1.2).

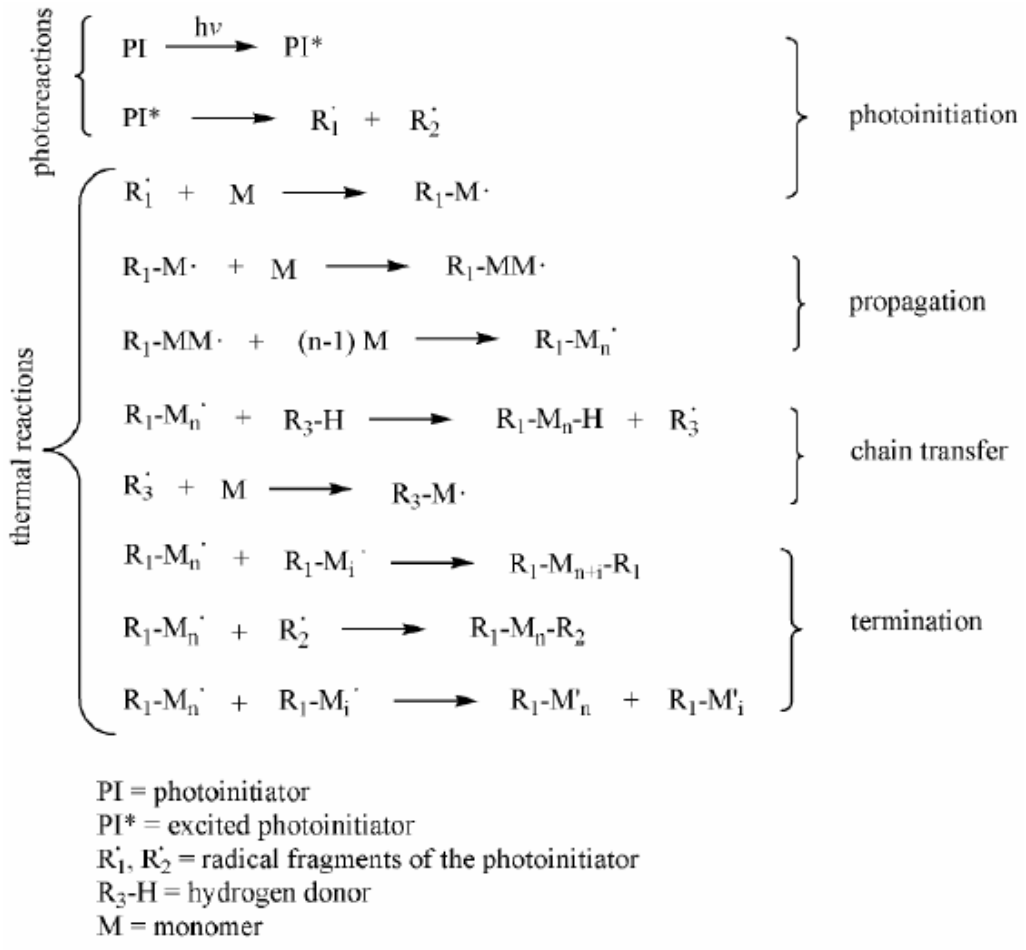

Figure 1.2. Steps of a photoinitiated free-radical polymerization.

Photoinitiation starts with the absorption of light by the photoinitiator or by the transfer of the energy again absorbed from light by a photosensitizer to the photoinitiator. This excitation leads to the dissociation of the initiator species to form radicals. Propagation is the process where the formed radicals react with the monomer to form the first macroradical which then repeatedly attacks to new monomers to form a long polymer chain with a radical ending [6]. A reaction in which the radical center is moved to another

compound (e.g. solvent or monomer) is known as chain transfer. The common type of this reaction is the shift of a hydrogen atom to the chain radical forming a new radical from the transfer agent while ending the ability to further grow for the previous molecule [8]. Termination is the step where the propagating polymer chain ceases to grow and terminates [9].

The rate of initiation for photopolymerization is given by

$$R_i = 2\Phi I_a \tag{1.1}$$

The factor of 2 in the equation above is used to indicate that two radicals are produced per molecule undergoing photolysis though 2 is not used when the initiating systems yield only one radical. Φ is the number of propagating chains initiated per light photon absorbed, also referred as the quantum yield for initiation. The maximum value of Φ is 1 for all photoinitiating systems. I_a is the intensity of absorbed light in moles of light quanta per liter-second.

The polymerization rate is obtained as

$$R_p = k_p[M](R_i / 2k_t)^{1/2} \tag{1.2}$$

where k_p stands for the propagation rate constant, [M] for the monomer concentration, R_i for the rate of initiation and finally k_t for the termination rate constant.
When equations 1.1 and 1.2 are combined the following equation is obtained.

$$R_p = k_p[M](\Phi I_a / k_t)^{1/2} \tag{1.3}$$

1.2. Monomers

A monomer molecule is defined as “A molecule which can undergo polymerization, thereby contributing constitutional units to the essential structure of a macromolecule” by IUPAC [10]. Acrylates and methacrylates are monomers predominantly preferred for radical polymerization because of the fact that their acrylic double bonds have higher reactivity compared to other double bonds [11]. These monomers are well-accepted for numerous applications, such as dental materials, biomaterials, coatings, polymeric membranes, microfluidic devices and stereolithography [12]. Despite their advantages (meth)acrylates still come with some limitations including polymerization shrinkage, residual unsaturation, photodegradation of the cured product due to the presence of initiator and oxygen inhibition. Acrylates are more susceptible to oxygen inhibition than methacrylates. This inhibition is caused by molecular oxygen reacting with carbon-based polymerizing radicals to form peroxy radicals which are noticeably less reactive towards double bonds, thus the efficiency of initiation is decreased. Also, atmospheric oxygen quenches excited triplet states of photoinitiators reducing the quantum yields of the initiating radicals [7]. Nitrogen-blanketing where the photopolymerization is performed under inert atmosphere is the most common method to overcome oxygen inhibition in photopolymerization [13]. Using impermeable films in order to avoid atmospheric oxygen is also a popular option.

Multifunctional acrylates such as hexanediol diacrylate, trimethylolpropane triacrylate or pentaerythritol tetraacrylate (Figure 1.3) are used to produce highly cross-linked, glassy polymer networks. These monomers lead to increased dimensional stability, high glass transition temperatures and reduced solvent absorption [14]. However, the highest conversion possible decreases since the mobility of the system decreases and the diffusion limitations to propagation increase [15].

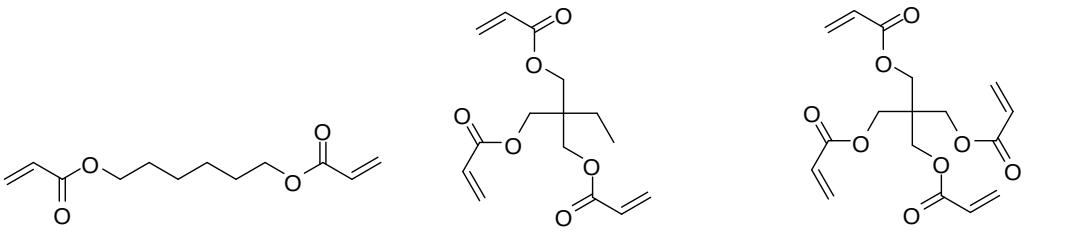

Figure 1.3. Structures of di-, tri- and tetra-functional acrylate monomers.

1.3. Light Sources

The light source used in photocuring is one of the main three constituents of photopolymerization including monomers and photoinitiators. The photoinitiating systems and the light sources should be chosen in a way that the spectral sensitivity of the former matches with the emission spectra of the lamp [16]. Some of the most common light sources such as mercury arc lamps, xenon lamps, excimer lamps, lasers, and light emitting diodes are explained below in detail.

1.3.1. Mercury Arc Lamps

By an electrical discharge in the Hg vapor excited levels are produced and the transitions between these excited levels and the ground state of mercury emit photons thus producing light. Mercury arc lamps produce particular lines and their intensities are related to the Hg pressure. For instance, low-pressure Hg lamps deliver photons around 254 nm and the emitted light is monochromatic whereas the medium-pressure ones give the spectrum shown in Figure 1.4 due to the fact that the frequency of the collisions of the mercury atoms have increased.

1.3.2. Xenon Lamps

Xenon lamps and also Hg lamps require high electrical power and give off a lot of heat but they emit a high light intensity over a wide spectral range. Unlike mercury lamps xenon lamps have their emission spectrum continuous in wavelengths [17] (Figure 1.4).

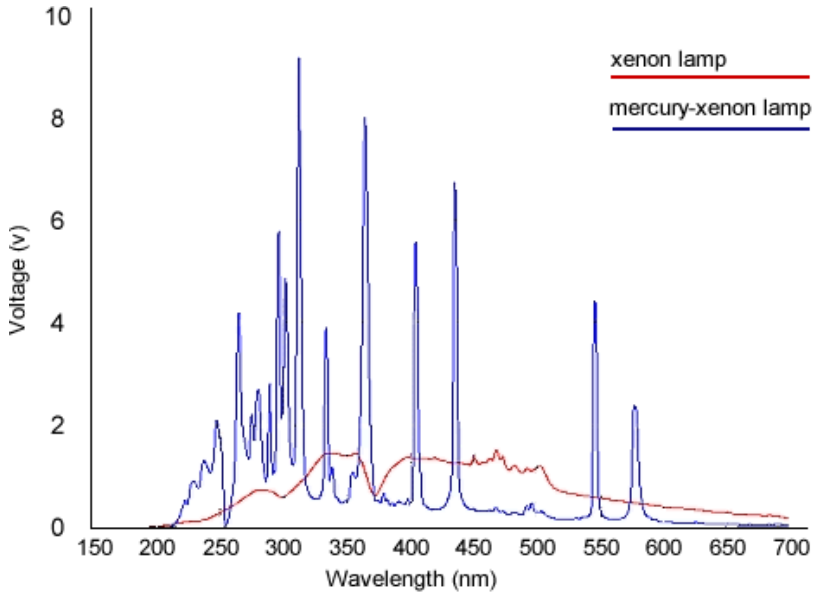

Figure 1.4. Typical spectral distributions for mercury and xenon lamps.

1.3.3. Lasers

Lasers have also been used widely in photopolymerization. They have various characteristics and benefits. Lasers are monochromatic light sources which allows control of light absorption, they have many different wavelength possibilities, their energy can be either delivered at a constant level as a function of time as in continuous-wave (CW) lasers or in a short time with pulsed lasers. Also, they deliver high concentration onto small surfaces which ensures a quasi-instantaneous curing and a reduced oxygen inhibition. The most preferred lasers include the following types:

- nitrogen lasers; λ = 337.1 nm
- excimer lasers; e.g., λ = 193, 248 nm
- helium-neon lasers; λ = 632.8 nm
- argon-ion lasers; e.g., λ = 363, 488, 514 nm
- Nd:YAG lasers; e.g., λ = 532 nm
- diode lasers; near IR wavelengths
- dye lasers, Ti:sapphire lasers ...

Lasers have a wide variety of power densities from a few hundred W cm^{-2} for continuous-wave lasers to a few MW cm^{-2} for pulsed lasers. When a CW laser is focused down to a spot size of 25 μm, the power density is increased to around 100 kW cm^{-2} for a laser that normally has a power of 500 mW.

1.3.4. Light Emitting Diodes (LEDs)

A light-emitting diode is a semiconductor device. LEDs have a spectral output which makes it possible to select an individual diode light source to provide the optimum excitation wavelength necessary. Also, new high-power LEDs are able to produce sufficient intensity, thus they are used in a wide range of applications. LEDs are known for their low heat generation, low energy consumption and low operating costs.

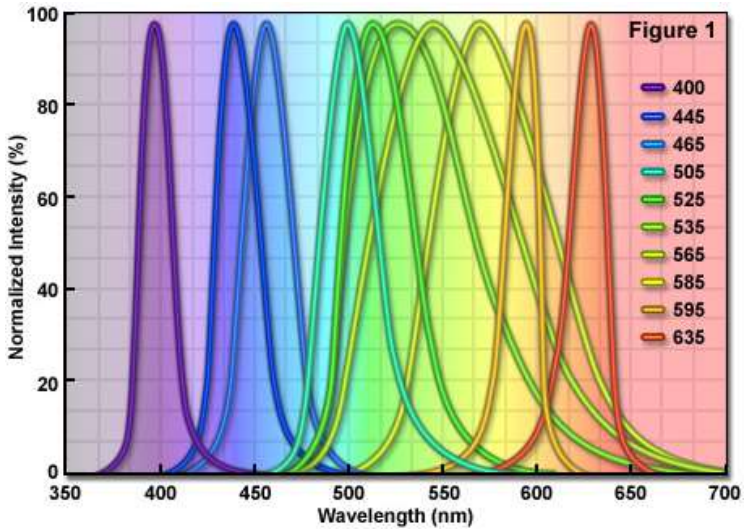

Figure 1.5. Spectral profiles of LEDs in visible range.

1.3.5. Excimer Lamps

Excimer lamps are discharge lamps. The emitted wavelength is a function of the gases that form the excimer. They are UV light sources for UV curing and they work at 308 nm or even at 222 nm or 172 nm in vacuum ultraviolet.

1.4. Free Radical Photoinitiators

The photoinitiator is a vital component of all radiation curable formulations. Photoinitiating systems are responsible for the efficient transformation of the energy of light into chemical energy in form of reactive species that are able to initiate the polymerization reaction [5].

Photoinitiating systems are expected to have some practical and intrinsic properties [18]. The practical requirements state that photoinitiators should not affect the final properties of the polymerized material. They should not lead to yellowing of photolysis products and have low sensitivity to air and moisture. Also, having good solubility or compatibility in the monomer/oligomer matrix is required. The intrinsic requirements are related to the reactivity of the PIs in terms of quantum yields. They include excellent light absorption qualities, reduced sensitivity to oxygen, excellent photochemical reactivity and high chemical reactivity of the initiating species.

Photoinitiators get excited and then lead to initiating radicals by the absorption of light. Upon irradiation electrons get excited from a bonding (π) or nonbonding orbital (n) to an antibonding orbital (π^*) (Figure 1.6). $n\pi^*$ transitions are between symmetry-different orbitals and thus symmetry-forbidden whereas $\pi\pi^*$ transitions occur between the π orbitals and so are symmetry-allowed transitions. The carbonyl group, RR'C=O, possesses all three types of orbitals: n orbital on the oxygen atom, π and π^* on the carbonyl double bond [19].

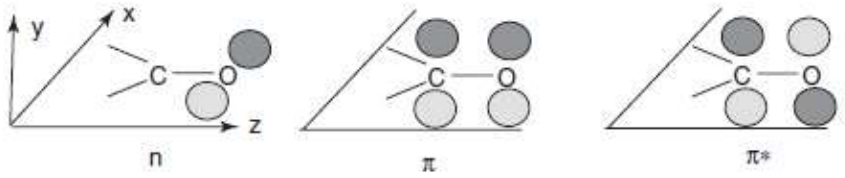

Figure 1.6. Three molecular orbitals that belong to the carbonyl group.

Irradiation transfers an electron from the ground state to an excited state, but this is possible only between states with the same multiplicity. Since ground states are singlet the

first excitation will generate excited singlet states (S_1, S_2 ...Sn) and the spin of the electron will remain the same. From there the excited molecule could either return to the ground state by internal conversion (e.g. fluorescence) or move to the triplet state by intersystem crossing. The radical formation occurs through cleavage of the excited molecule on the triplet state (Figure 1.7). For high initiation, the singlet and triplet states need to have lifetimes as short as nanoseconds so that quenching reactions are avoided.

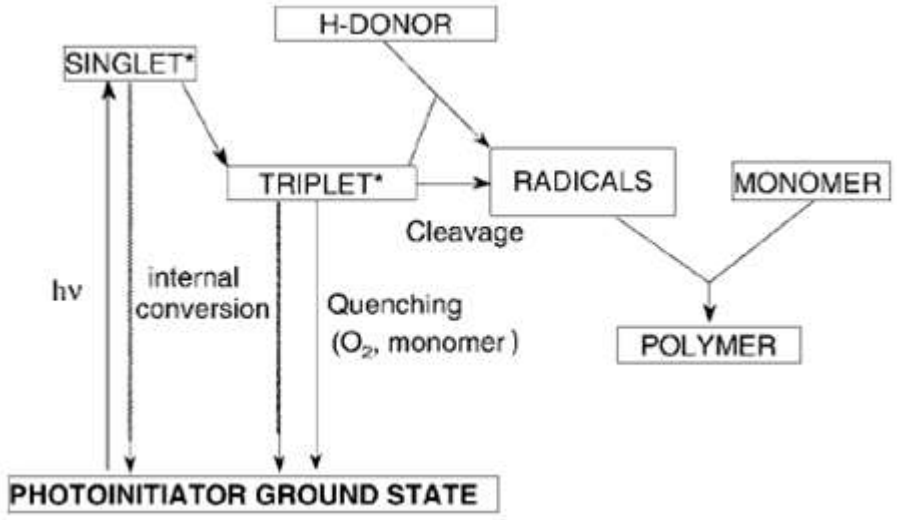

Figure 1.7. Various pathways for the excited photoinitiator molecule [20].

Photoinitiators are responsible for controlling both the reaction rate through the quantum yield of formation of initiating species and the penetration of incident radiation through its light absorbance. Therefore, it is important to choose the photoinitiator wisely so it demonstrates the highest initiation efficiency and also undergoes fast photobleaching upon UV exposure to achieve a deep-through cure.

Radical formation from photoinitiator molecules can occur *via* two possible reaction processes one based on cleavable (Type I) and the other on non-cleavable (Type II) compounds (Figure 1.8).

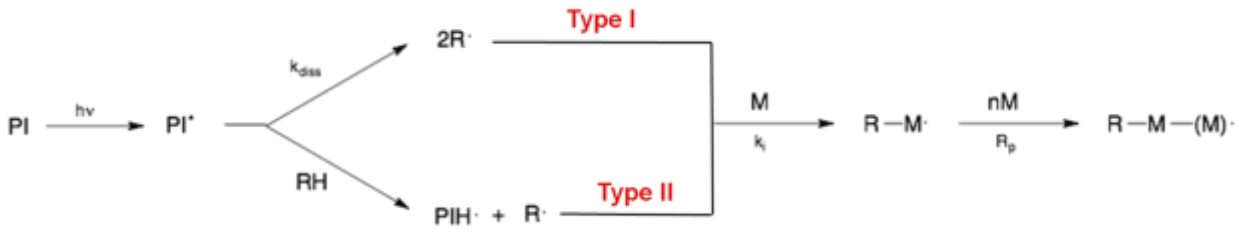

Figure 1.8. Possible reaction processes of photoinitiators.

1.4.1. Type I Photoinitiators

Type I photoinitiators undergo homolytic cleavage upon irradiation and decompose into radicals (Figure 1.9). The α-cleavage type photoinitiators only require light in order to form radicals; therefore, Type I initiators have a generally higher efficiency.

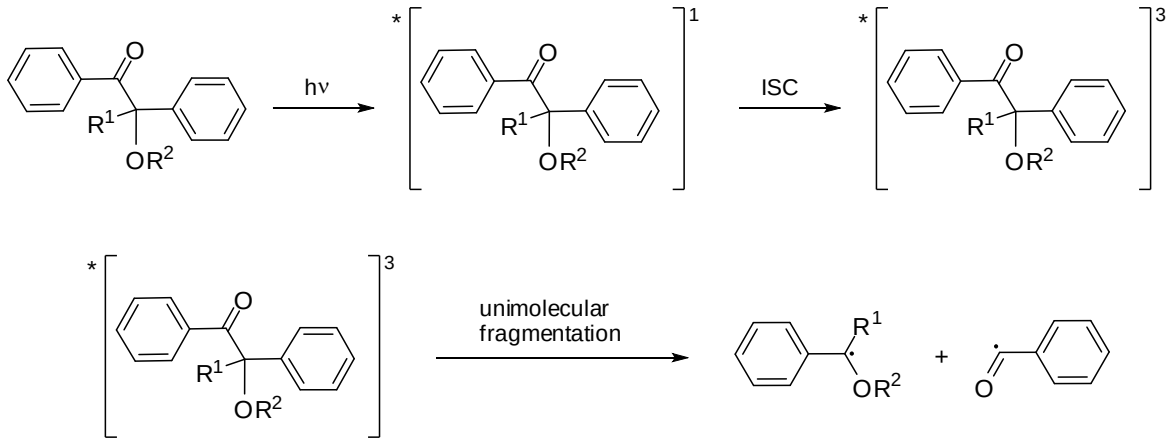

Figure 1.9. Homolytic cleavage reaction of a Type I photoinitiator.

Most of the efficient Type I photoinitiators are based on the benzoyl chromophore and absorb in the UV range. It is essential for a photoinitiator to have bond energies lower than the energy of the light source so that the irradiation would provide enough enery to break the necessary bond. The CO-alkyl bond energy is around 65-70 kcals/mol which is less than the usual amount of energy that a UV light provides (70-80 kcals/mol), allowing the photoinitiator to go through the cleavage reaction on its own [21]. Absorption

properties of some Type I photoinitiators that are based on benzoin ether derivatives are given in Table 1.1 [19].

Table 1.1. Absorption properties of different Type I photoinitiators in n-hexane [19].

	λ_{max} (nm)	ε_{max} (mol^{-1} l cm^{-1})	ε_{366} (mol^{-1} l cm^{-1})
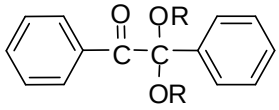 DMPA	343	230	117
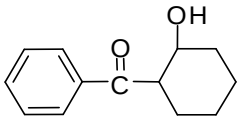 HCAP	311	93	9
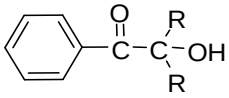 HAP	305	260	5
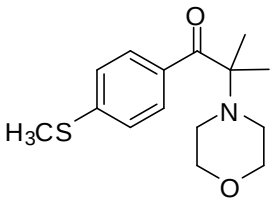 TPMK	300	13000	70
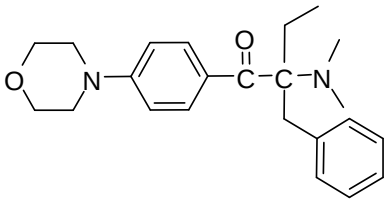 MPPK	308	20900	270

1.4.2. Type II Photoinitiators

Type II photoinitiators are subjected to excitation and the excited species interact with a second compound to form radicals, thus they undergo bimolecular reactions which make them slower than Type I photoinitiators. Most known Type II photoinitiators are

based on benzophenone (BP), thioxanthone (TX), camphorquinone (CQ) and anthraquinone (AQ) (Figure 1.10) [22].

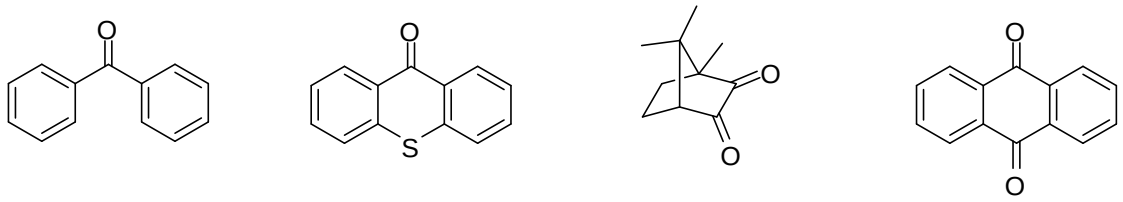

Figure 1.10. Examples of Type II photoinitiators.

Type II photoinitiators work in their excited triplet state by a primary electron transfer in the presence of an amine, which is then followed by a proton transfer. The primary process is fast if proper amines are selected and it could compete with monomer quenching. Another way Type II photoinitiators work is by hydrogen abstraction reaction in the presence of a hydrogen donor such as an alcohol, tetrahydrofuran (THF) or even a polymer chain that possesses labile hydrogens. Only nπ* triplet states can react through hydrogen abstraction reaction and due to their longer triplet state lives these reactions are susceptible to quenching reactions (Figure 1.11).

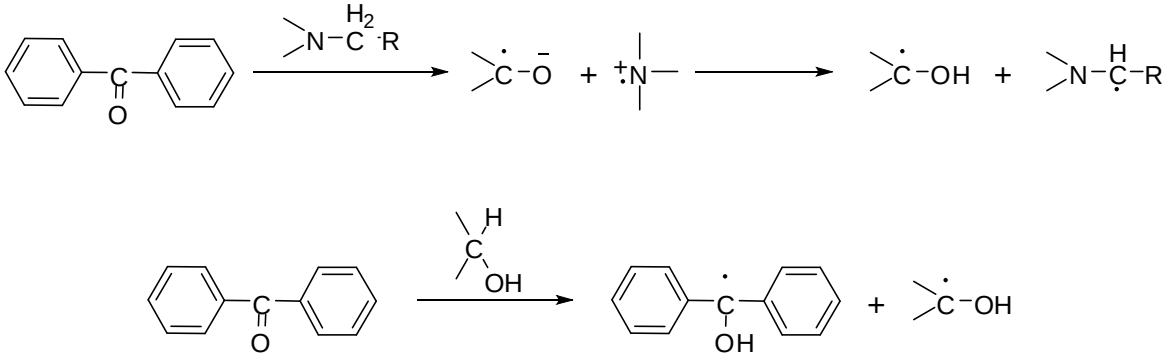

Figure 1.11. Radical formation reactions for Type II photoinitiators [22].

The ketyl radicals formed in the above reactions are known as terminating agents because of their lack of reactivity towards the growing polymer chain due to steric

hindrance, delocalization of the unpaired electron and their tendency to give side products whereas the alkyl radicals are the initiating radicals.

The most well-known coinitiators are amines that are aliphatic or aromatic which could be secondary or tertiary (Figure 1.12). Aliphatic amines are transparent down to 260 nm hence allow use of light from the UV lamp in this range. On the other hand the aromatic amines show strong absorption around 300 nm and thus screen much of the UV light [23]. Therefore, when curing with benzophenone using aliphatic amine is favorable, whereas thioxanthones, due to their strong absorption at wavelengths greater than 400 nm, can be used successfully with an aromatic amine. Tertiary amines are more reactive than alcohols or ethers; and thiols are another type of coinitiators used in thiol-ene photopolymerization systems [3].

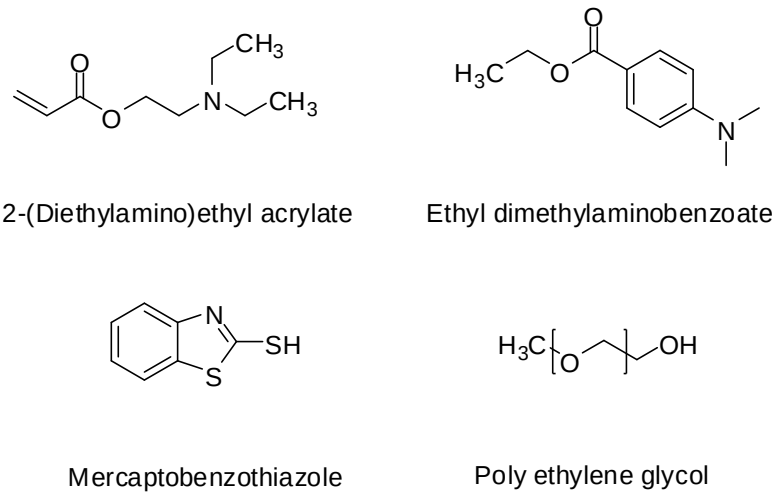

2-(Diethylamino)ethyl acrylate

Ethyl dimethylaminobenzoate

Mercaptobenzothiazole

Poly ethylene glycol

Figure 1.12. Examples of coinitiators.

1.4.3. Photoinitiators containing both Type I and Type II units

Radiation curing is a well-established technology however it still requires appropriate tuning of its components to fit special applications [24]. The efficiency of conventional photoinitiators is known to be low at times due to the fact that only a small region of the incoming light is absorbed by it and a fraction of the absorbed light is useful for forming reactive species that initiate the photopolymerization. To overcome this

handicap, photosensitizers could be used so that the free radicals can be produced not only by the direct excitation of the photoinitiator but also by energy transfer from a photosensitizer to the photoinitiator (Figure 1.13).

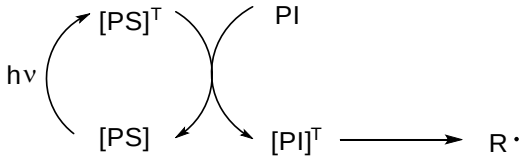

Figure 1.13. Radical generation by sensitization [24].

In order to achieve an efficient sensitization a close contact of the photosensitizer and the photoinitiator is required. For this purpose three different photoinitiating systems were prepared in the literature containing both the photoinitiator (Type I) and the photosensitizer (Type II): 1-{4-[2-(4-benzoyl-phenoxy)-ethoxy]-phenyl}-2-hydroxy-2-methyl-propan-1-one (**1**), 2-benzoyl benzoic acid 2-[4-(2-hydroxy-2-methyl-1-oxopropyl)phenoxy]ethyl ester (**2**) and thioxanthone-1-carboxylic acid 1-[1,1-dimethyl-2-(4-methylsulfanyl-phenyl)-2-oxo-ethyl]-piperidin-4-yl ester (**3**) (Figure 1.14) [24].

The UV absorption spectra of these photoinitiators were measured and compared with their constituents in order to analyze the interaction between the two components forming the photoinitiators (Figure 1.15). The absorption maximum of the covalently bonded initiator **1** was found at 283 nm which is between the λ_{max} values of the components α-hydroxyalkylphenone (**4**) and 4-hydroxybenzophenone (**5**) (Figure 1.14). The same result is valid for the extinction coefficients which prove that there is an interaction between the two segments because otherwise the extinction coefficient in a two-component system would be additive. It is clear in the figure that in the region of the ππ* transition there is an interaction of the chromophores.

Additionally, the photo-DSC studies of the photoinitiators were carried at 365 nm under nitrogen and air (Figure 1.16). The covalently bonded photoinitiator gave a higher rate of polymerization (R_p) than its physical mixture counterpart under both nitrogen and air.

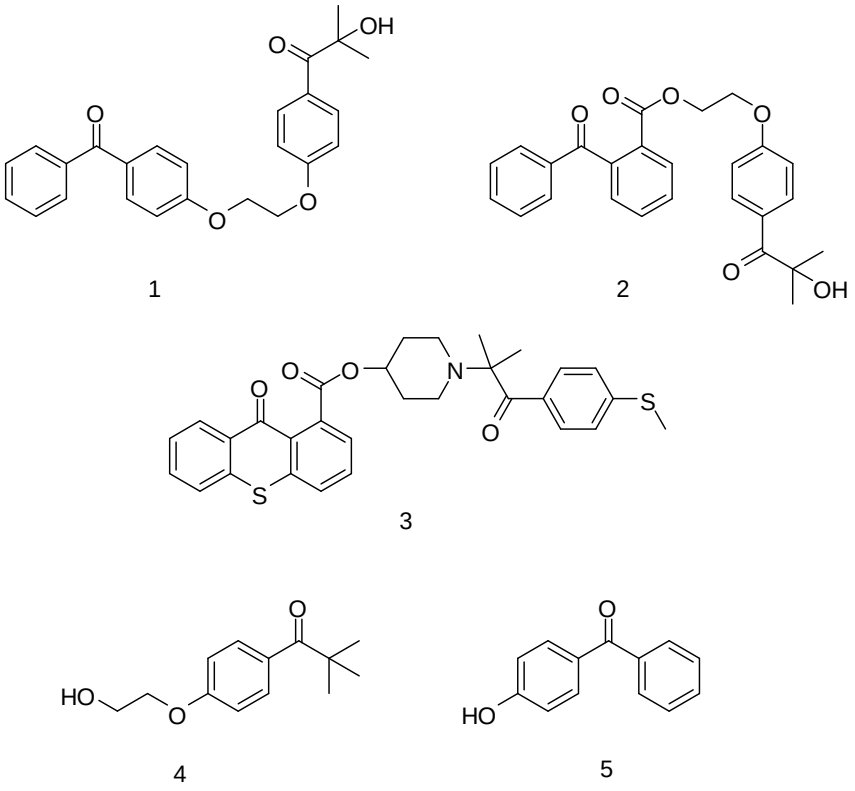

Figure 1.14. New photoinitiators with nonconjugated chromophores [24].

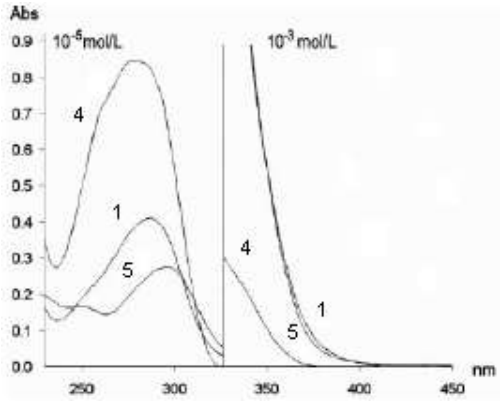

Figure 1.15. UV spectra of 1, 4 and 5 in methanol (1×10^{-5} and 1×10^{-3} mol/L).

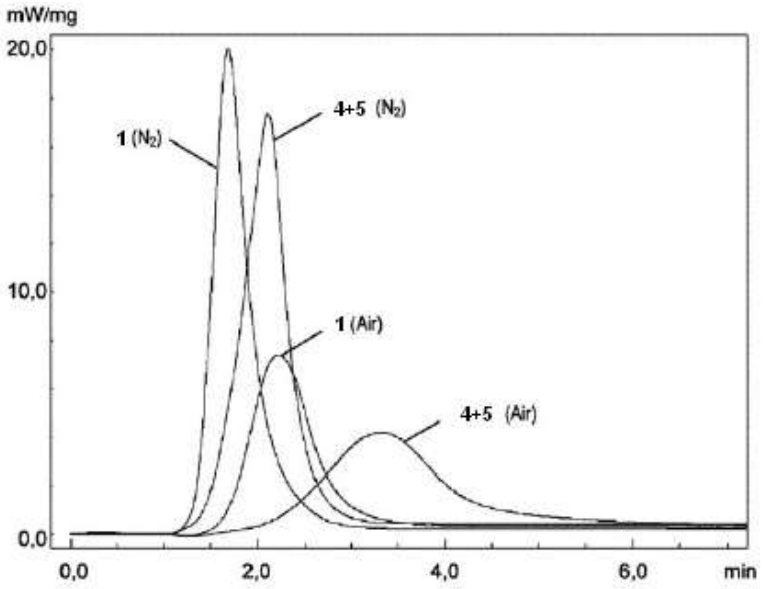

Figure 1.16. Photo-DSC (365 nm) of HEA with 1 and a mixture of 4 and 5 as PIs.

The photosensitization process is especially useful when the sensitizer can be excited with light of different wavelengths than the photoinitiator [25]. For this purpose three different photoinitiators have been synthesized where the photosensitizer component is a thioxanthone derivative that absorbs light under visible light and the photoinitiator part absorb UV light (Figure 1.17).

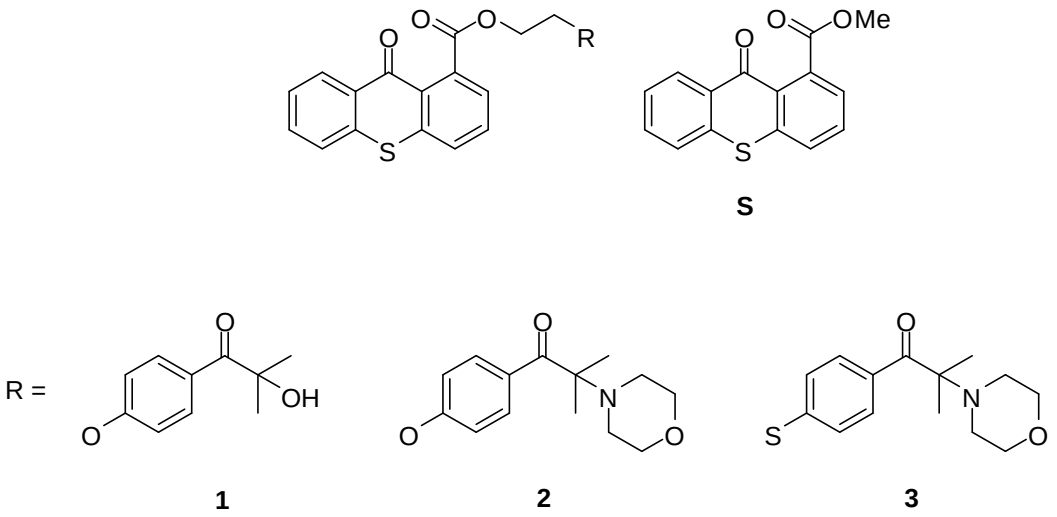

Figure 1.17. Three novel photoinitiators and their reference sensitizer [25].

The triplet energy of the sensitizer needs to be higher (or approximately the same in some cases) than the photoinitiator in order to be able to transfer its energy and lead to radical formation. Therefore, the efficiency of **1** does not differ from P1 (see Figure 1.18) due to S having a substantially lower triplet energy compared to P1. However, the half-life of the triplet states of **2** and **3** are affected by the covalent bonding of S and the respective initiators. The intramolecular triplet energy transfer is considerably slower for **2** than for **3** which is in line with their triplet energies.

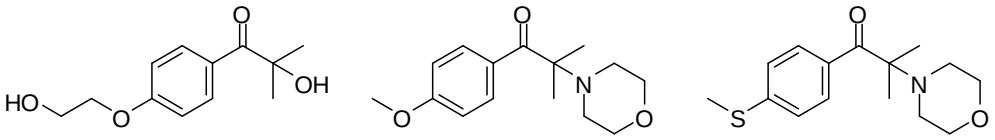

PI1 **PI2** **PI3**

	E_T (kcal · mol^{-1})
S	63
PI1	71
PI2	65
PI3	61

Figure 1.18. References of the photoinitiating units of 1, 2 and 3 and their triplet energies [25].

1.5. Monomeric and Polymeric Photoinitiators

The traditional small-molecule photoinitiators suffer from migration of the unreacted photoinitiator molecules from the cured samples to the surface of the material and eventually into the surrounding medium. Such migration would lead to toxicity in food packaging or biomedical uses. Furthermore, low-weight photoinitiators may bring in yellowing and/or odor. One important way to get rid of these drawbacks is to develop macrophotoinitiators which have advantages over low-molecular weight analogues. Therefore, polymerizable, dendritic, hyperbranched or polymeric photoinitiators have been developed with higher activity, greater curing speed and low migration rate which also results in low odors, non-toxicity and less yellowing [26-57].

Numerous novel macrophotoinitiators have been studied containing the photofragmenting (Type I) and hydrogen-abstracting (Type II) chromophores. Benzoin derivatives, benzyl ketals, acetophenone derivatives are the most popularly used Type I moieties, whereas BP, TX or CQ are Type II photoinitiating groups.

Benzophenone is highly preferred photoinitiator because of its many advantages such as good surface curing property, good oxygen inhibition effect and good solubility properties. Coinitiators are a fundamental part of benzophenone-based photoinitiators and they could either be electron/proton donors or hydrogen donors.

Polyethylene glycol (PEG) has drawn attention due to its good hydrophility and hydrophobility therefore forming a polymeric photoinitiator with a PEG chain gives the photoinitiator a good compatibility in both oil and water. Benzophenone-based Type II polymeric photoinitiators PEG-BP were synthesized with different molecular weights (Figure 1.19). The PEG-BP systems were proven to give the same conversion as a BP/EDAB mixture. Thus, the pronounced advantage of this initiator is the elimination of amine based hydrogen donors and being easily available as well as non-toxic [26].

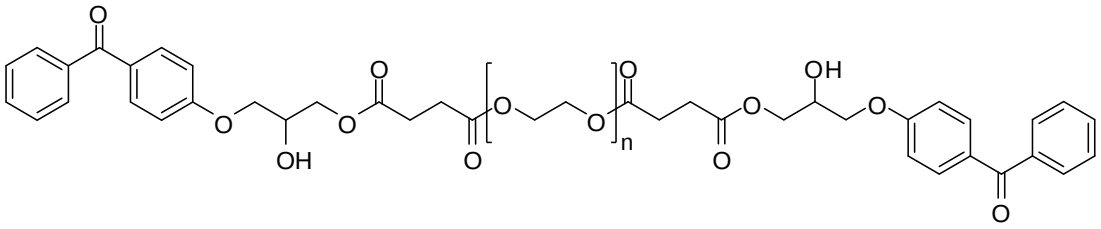

PEG-BP

Figure 1.19. Polymeric photoinitiator containing BP and PEG moieties [26].

Sesamol is known to be a good hydrogen donor so a molecule (BDOPAc) has been synthesized with benzophenone and sesamol that is also polymerizable (Figure 1.20). The rate of decomposition and the migration stability of the photoinitiator have been studied and compared with its references. The results showed that this new photoinitiator is effective for radiation curing and has a lower amount of leachable photoinitiator than the BP/EDAB mixture. The introduction of BDOBPAc has opened a way to decrease or

eliminate the use of amines making it convenient for food packaging or biomedical fields [27].

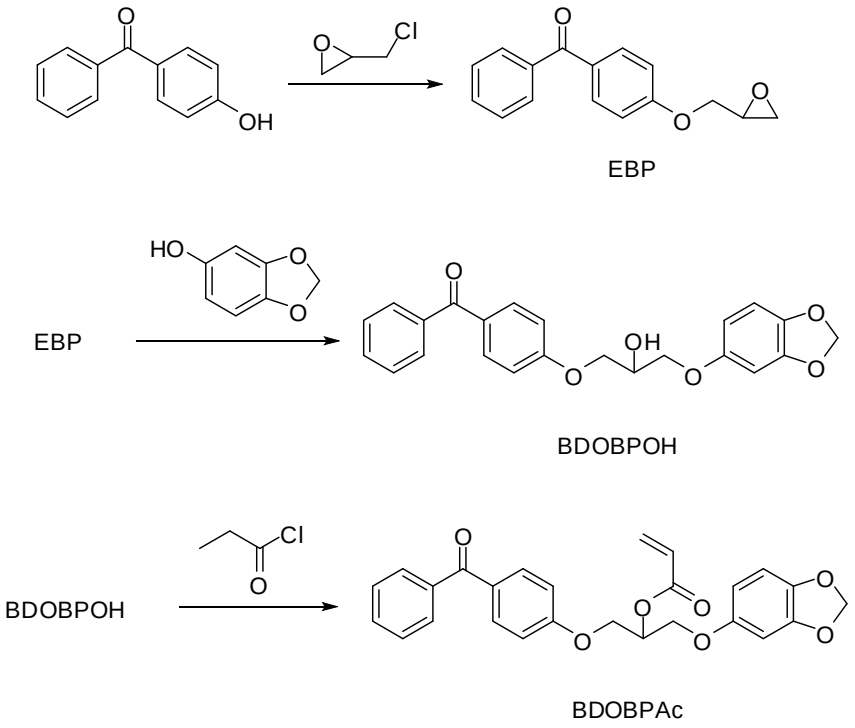

Figure 1.20. The synthesis route of BDOPAc [27].

Dendritic poly (propylene imine) is highly branched and it could be used as a hydrogen donor therefore, introducing thioxanthone and the vinyl monomer into the system could bring some advantages by eliminating the use of low molecular weight amines due to the possibility of intramolecular energy transfer between the thioxanthone and amine. Three dendritic macrophotoinitiators have been produced and the photopolymerization behaviors with monofunctional monomer methyl methacrylate (MMA) and trifunctional monomer trimethylolpropane triacrylate (TMPTA) have been studied (Figure 1.21). DAB-64-TX-OC is the most efficient photoinitiator for MMA but due to diffusion control for TMPTA DAB-16-TX-OC is proved to be the most efficient one [28].

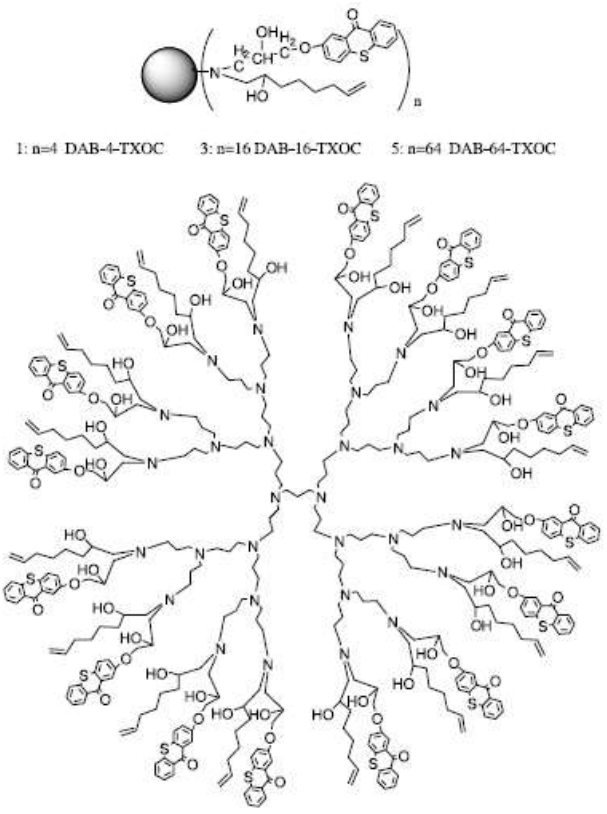

Figure 1.21. Three kinds of copolymeric dendritic macrophotoinitiators [28].

Camphorquinone is widely used in dentistry as initiating agent in the photocuring of restorative dental composite resins upon irradiation with visible light. Camphorquinone behaves as a Type II photoinitiator and works in a good alliance with tertiary amines. Novel polymethacrylic photoinitiators bearing photosensitive camphorquinone and/or tertiary amine in the side chain has been synthesized (Figure 1.22). The system formed by polymeric camphorquinone and a low-molecular weight amine has showed a slightly higher conversion than all-low molecular weight combination. Also, when the camphorquinone was low molecular weight and the amine was polymeric, the system still gave a similar conversion result to (1R)-10-pivaloyloxy-camphorquinone/2-(Dimethylamino)ethyl pivalate (PCQ/DMAEP) mixture. When both photoreactive moieties are polymeric and in the case of the copolymeric photoinitiator, containing both the camphorquinone and amine groups in the side chain, the rate drops compared to the previous systems and this is attributed to the steric hindrance to exciplex formation [29].

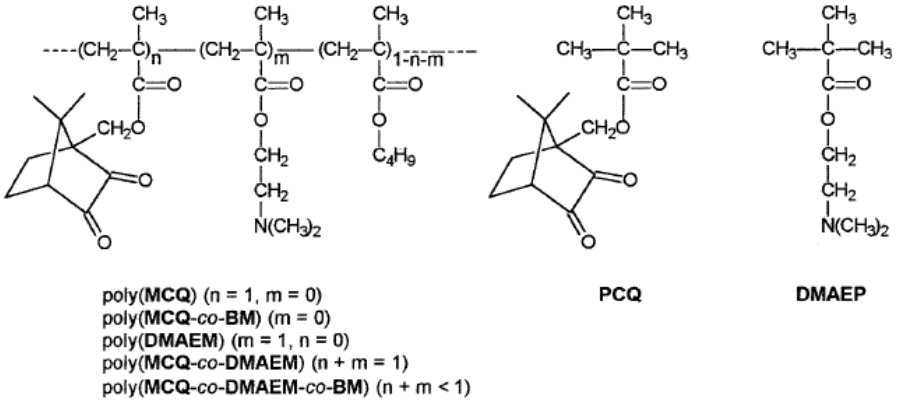

Figure 1.22. Structures of novel polymeric and low molecular weight photoinitiators [29].

Benzoin ethers are particularly convenient and thus used in several Type I applications under UV-light irradiation. In order to study their behavior upon irradiation two polymeric photoinitiators having benzoin methyl ether moieties linked to the main chain through the α-methylol group and to the carboxy group through the para position of the benzyl ring have been synthesized (Figure 1.23). The former gives rise upon irradiation to the low molecular weight benzoyl radical and the polymer-bound α-alkoxybenzyl radical whereas the latter produces the reverse situation and forms the polymer-bound benzoyl radical and a low molecular weight α-alkoxybenzyl radical. Since benzoyl radicals are more active as initiating species than α-alkoxybenzyl radicals which are involved mostly in the termination reactions, the former polymeric photoinitiator reacts more effectively upon irradiation due to having the benzoyl radical in low molecular weight form, which increases its mobility compared to the polymeric radical [30].

Phenyl-substituted phosphine oxides are available for wavelengths up to 420 nm and therefore are drawing attention for biomedical uses where UV light might be damaging. Three vinyl-functionalized phosphine oxide photoinitiating monomers have been synthesized and these monomers have been further copolymerized with dimethylacrylamide to yield polymeric photoinitiators containing acylphosphine oxide groups (Figure 1.24). The polymeric photoinitiator derived from the first monomer turned out to be not stable in water so, methyl groups were added to the aromatic ring in order to inhibit nucleophilic attack and hence the second monomer was formed. When the two polymeric photoinitiators synthesized from the second and third monomers were

compared, the polymeric photoinitiator releasing a low molecular weight phosphinoyl oxide radical appeared to be more effective in polymerization than the one forming a low molecular weight benzoyl radical upon irradiation justifying that the phosphinoyl radical is more effective than the benzoyl radical [31].

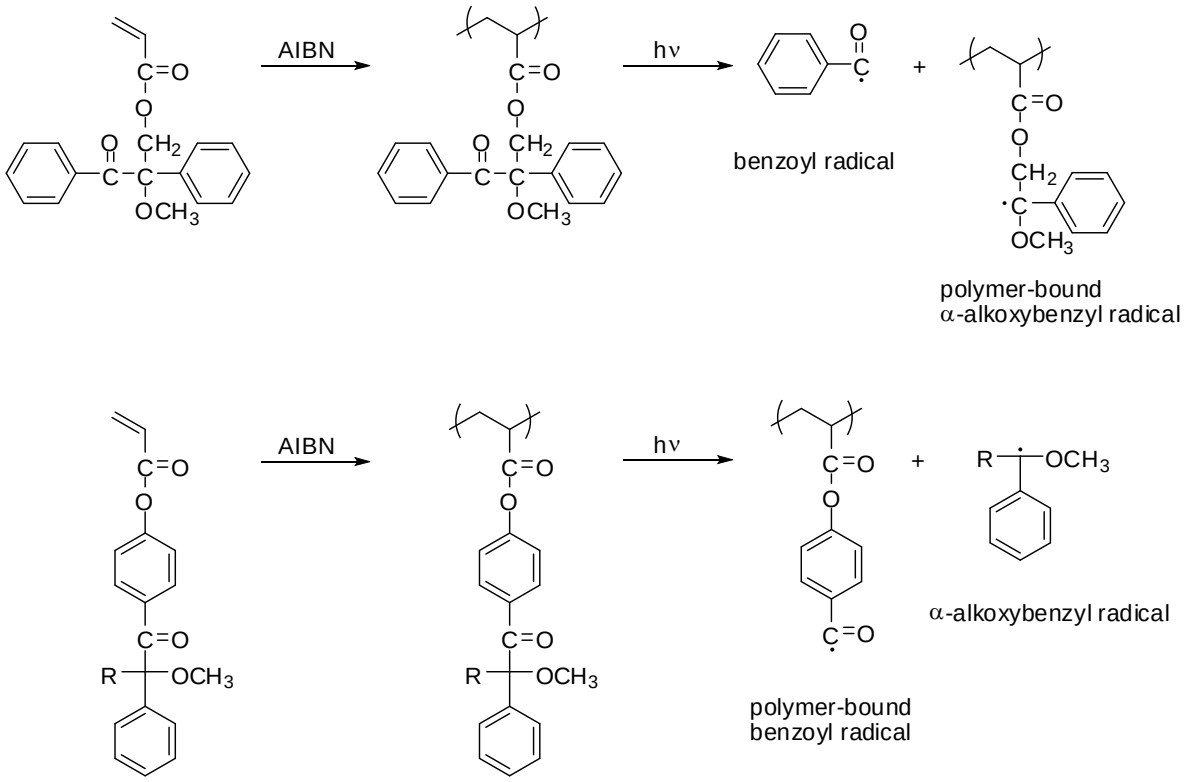

Figure 1.23. Photofragmentation process for PPIs containing benzoin methyl ether moieties [30].

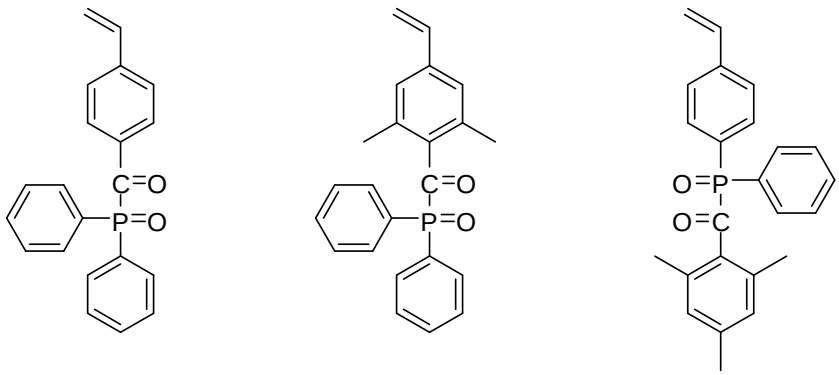

Figure 1.24. Three vinyl phosphine oxide photoinitiator monomers [31].

When UV curing fails to be sufficient for a photopolymerization for instance in some cases of pigmented coating, thioxanthone might be used as a photoinitiator since it absorbs light around 380 nm (visible light). However due to thioxanthone requiring amines to work which generates yellowing, a polymeric photoinitiator containing both thioxanthone (Type II) and α-morpholino-acetophenone (Type I) on the side-chains has been synthesized in order for it to work by energy transfer between the moieties (Figure 1.25). The thioxanthone part of the polymer acting as a photosensitizer absorbs the visible light thus getting excited and transfers its energy to the α-morpholino-acetophenone moiety leading to the formation of radicals without the presence of an amine. For an energy transfer this kind both the photoinitiators and photosensitizers have to be close to each other so energy transfer is favored [32].

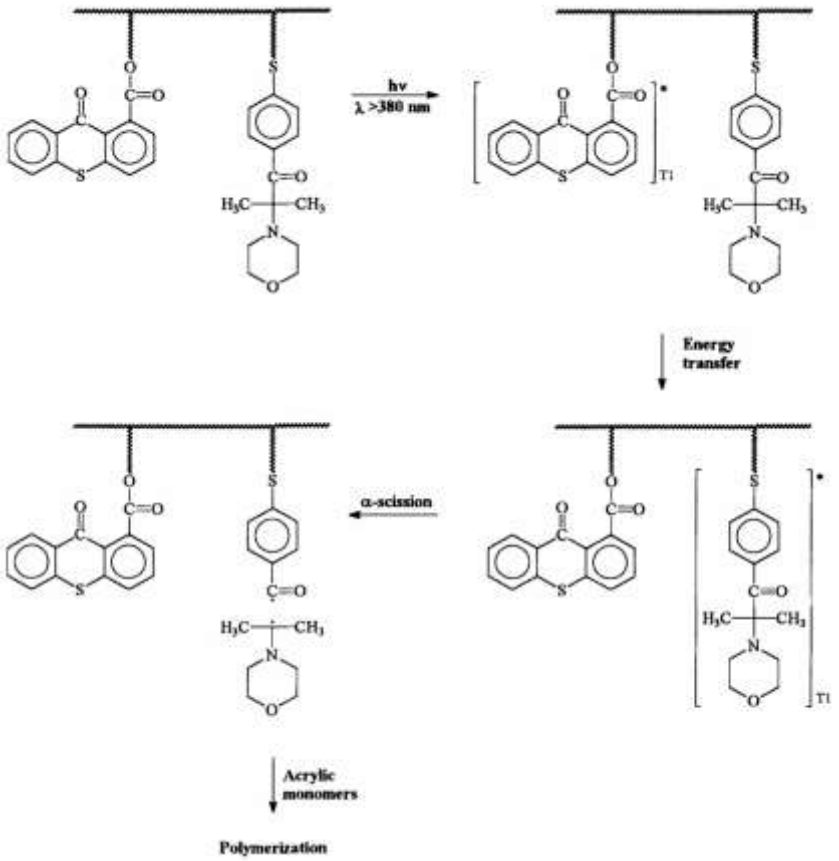

Figure 1.25. The representation of the intramolecular excitation energy transfer from the TX triplet state to the ground state α-morpholino-acetophenone chromophore [32].

2. OBJECTIVES

The objective of this study is to prepare novel monomeric and polymeric photoinitiators i) containing both Type I (Irgacure 5959) and Type II (BP or TX) photoinitiating groups to investigate the effectiveness of photoinitiator and photosensitizer being in close contact; ii) containing both BP photoinitiating and hydrogen donor (sesamol) groups in their structures to exclude toxic amines.

The copolymerization of these monomeric photoinitiators with butyl methacrylate gives novel polymeric photoinitiators. The photoefficiencies of each photoinitiator in the polymerizations of HDDA are explored using real-time FTIR and compared with commercial BP, TX and Irgacure 2959.

3. EXPERIMENTAL WORK

3.1. Materials and Characterization

3.1.1. Materials

The following analytical-grade chemicals were obtained from commercial sources and used without further purification: hexane-1,6-diol diacrylate (HDDA), 4-hydroxybenzophenone, thioxanthen-9-one, pyridine, Irgacure 2959, sesamol, 2,2'-azobis(isobutyronitrile) (AIBN), butylmethacrylate (BMA), N,N-dimethylaminoethyl methacrylate (DMAEM), *tert*-butyl acrylate, paraformaldehyde, 1,4-diazabicyclo[2.2.2]octane (DABCO) from Aldrich Chemical Co.; benzophenone, sodium sulfate, oxalyl chloride, chloroform and all other solvents were purchased from Merck. Dimethylformamide (DMF) and dichloromethane (DCM) which were also obtained from Merck were dried over activated molecular sieves.

3.1.2. Characterization

^{1}H and ^{13}C-NMR spectra were obtained on a Varian Gemini (400 MHz) spectrometer. For Infrared spectral analysis a Nicolet 6700 FTIR spectrophotometer was used. Photopolymerizations were performed using the same instrument. The glass transition temperatures were obtained using a TA Instruments Q100 differential photocalorimeter (DPC), under nitrogen atmosphere at a heating rate of 10 °C/min. The UV-Vis spectra were obtained by using a Shimadzu UV-2450 spectrophotometer.

3.2. Synthesis of starting materials

3.2.1. Synthesis of TBHMA

This monomer was synthesized according a to literature procedure [58]. *tert*-Butyl acrylate (127.7 g, 0.99 mol, 146 mL), paraformaldehyde (30 g), 1,4 Diazobicyclo [2.2.2]

octane (DABCO) (14 g, 0.13 mol), dimethyl sulfoxide (225 mL) and water (85 mL) were added into a 1000 ml round-bottom flask which was attached to a condenser and places in a preheated oil bath at 96-98 °C. The solution was refluxed under nitrogen for 30 min, and then it was cooled. The solution was first divided into two and the first half was extracted with 1wt% HCl (2 x 35 mL), the organic phase was combined with the other half of the solution and extracted with 1wt% HCl (2 x 65 mL), dried with anhydrous $CaCl_2$ and filtered. The excess *tert*-butyl acrylate was evaporated and the remaining solution was distilled under reduced pressure in the presence of a free radical inhibitor. $CuCl_2$, and pure TBHMA as a colorless liquid was collected at 60-65 °C in 18 per cent (27.29 g) yield.

^{13}C-NMR (400 MHz, $CDCl_3$, TMS): δ = 28.1 (CH_3), 62.4 (CH_2-O), 81.2 [*C*-(CH_3)$_3$], 124.4 (*C*H_2=C), 140.6 (*C*=CH_2), 165.4 (*C*=O) ppm.

^{1}H-NMR (400 MHz, $CDCl_3$, TMS): δ = 1.49 (CH_3), 2.68 (O-H), 4.25 (CH_2-O), 5.72 (CH=C), 6.12 (CH=C) ppm.

FT-IR: 3420 (OH), 2978-2934 (C-H), 1709 (C=O), 1639 (C=C), 1457-1369 [C-(CH_3)$_3$], 1159-1054 (C-O) cm^{-1}.

3.2.2. Synthesis of TBBr

This monomer was synthesized according a to literature procedure [59]. TBHMA (27.29 g, 0.1725 mol), and ether (165 mL) were placed in 500 mL round-bottom flask. PBr_3 (8 mL) was added dropwise to the solution in an ice bath. Nitrogen gas was purged to remove HBr gas that evolves during the reaction. After complete addition, the solution was allowed to warm to room temperature and stirred for three hours under nitrogen at room temperature. Then, 110 mL of water was added dropwise to the solution in an ice bath. The aqueous phase was separated and extracted with hexane (2 x 35 mL), then the organic phases were combined and washed with saturated NaCl solution (Brine) (2 x 35 mL), dried with anhydrous Na_2SO_4 and filtered. After removal of ether by rotary evaporator, distillation under reduced pressure in the presence of $CuCl_2$ gave TBBr as a colorless liquid at 40-50 °C head temperature.

^{13}C-NMR (400 MHz, $CDCl_3$, TMS): δ = 27.9 (CH_3), 29.7 (CH_2-Br), 81.5 [*C*-(CH_3)$_3$], 127.8 (*C*H_2=C), 138.8 (*C*=CH_2), 164.1 (C=O) ppm.

^{1}H-NMR (400 MHz, $CDCl_3$, TMS): δ = 1.47 (CH_3), 4.09 (CH_2-Br), 5.79 (CH=C), 6.16 (CH=C) ppm.

FT-IR: 2978-2934 (C-H), 1718 (C=O), 1621 (C=C), 1226-1158 (C-O), 720 (C-Br) cm^{-1}.

3.3. Synthesis of PI1 & PI2

3.3.1. Synthesis of Synthesis of TBBr-BP

This monomer was synthesized according to a literature procedure [35]. To a mixture of 4-hydroxybenzophenone (1.43 g, 7.2 mmol) and K_2CO_3 (10.32 g, 74.7 mmol) in acetone (15 mL) under nitrogen, TBBr (1.73 g, 7.8 mmol) was added dropwise in an ice bath. The solution was placed in an oil-bath that was preheated to 60 °C for 48 hours. Then, the solvent was removed by rotary evaporator. Dichloromethane (15 mL) was added to the remaining solid and the solution was first extracted with water (3 x 10 mL) and then with 5% NaOH (3 x 10 mL). The organic phase was dried over anhydrous Na_2SO_4, filtered and the remaining solvent was evaporated. Residue was purified by re-crystallization from methanol. The pure product was obtained as a white solid (mp 53-54 °C) in 51% yield.

^{13}C-NMR (400 MHz, $CDCl_3$, TMS): δ = 28.0 (CH_3), 66.5 (CH_2-O), 81.5 (*C*-CH_3), 114.5 (Ar-CH), 125.7 (C=*C*H_2), 128.1 (Ar-CH), 130.4 (Ar-CH), 131.9 (Ar-C), 132.5 (Ar-CH), 132.7 (Ar-CH),136.7 (Ar-C), 138.7 (*C*=CH_2), 161.9 (Ar-C), 164.5 (C=O ester), 195.6 (C=O ketone) ppm.

^{1}H-NMR (400 MHz, $CDCl_3$, TMS): δ = 1.5 (9H, s, CH_3), 4.8 (2H, s, CH_2-O), 5.9 (1H, s, CH_2=C), 6.3 (1H, s, CH_2=C), 6.9 (2H, d, Ar-CH), 7.5–7.8(7H, m, Ar-CH) ppm.

FTIR (ATR): 2976 (C-H), 1713 (C=O), 1680(C=O), 1142 (C=O) cm^{-1}.

3.3.1. Synthesis of TBBr-BP-CA

This monomer was synthesized according to a literature procedure [36]. TFA was added dropwise to TBBr-BP in an ice bath under nitrogen. The mixture was stirred at room temperature for 24 h. After removal of excess TFA, the remaining solid was washed with diethyl ether and filtered. The remaining pure white solid was dried in a vacuum oven and gave a yield of 47% (mp 70-71 °C).

3.3.2. Synthesis of PI1

TBBr-BP-CA (0.33 g, 1.072 mmol) was purged with nitrogen for 15 minutes. Dry CH_2Cl_2 (1.28 mL) was added. Then the mixture of oxalyl chloride (0.74 g, 0.5 mL) and dry CH_2Cl_2 (1.88 mL) was added dropwise under ice bath and nitrogen. Ten drops of solution (1 mL of CH_2Cl_2 and 0.2 mL of dimethylformamide) was added and the reaction mixture was stirred for half an hour in an ice bath under nitrogen. After half an hour, ice bath was removed and the reaction was stirred for another three and half an hour at room temperature. The solvent and excess oxalyl chloride were evaporated with nitrogen and the remaining acid chloride was used in the next step.

To the solution of the acid chloride (0.35 g, 1.072 mmol) in 2.70 mL of dry dichloromethane, Irgacure 2959 (0.27 g, 1.18 mmol) was added at room temperature. Then a solution of 2.15 mL of dry dicholoromethane and pyridine (0.095 mL (0.094 g), 1.18 mmol) was added in an ice bath. The reaction went on for 2.5 hours at room temperature. Once the reaction was over the solution was mixed with 30 mL of dichloromethane and was first extracted with water (2 x 9 mL) and then with $NaHCO_3$ (2 x 9 mL). The organic phase was dried over with sodium sulfate, filtered and the solvent was evaporated. The remaining oily substance was purified *via* column chromatography on silica gel 60 (70-230 mesh) using hexane initially and gradually changing to ethyl acetate as eluent.

^{13}C NMR (400 MHz, $CDCl_3$, TMS): δ = 28.53 (CH_3), 65.83, 66.08, 75.96 (CH_2-O), 78.11 (Ar-C), 114.10 (Ar-CH), 126.42 (*C*H_2=C), 128.15 (Ar-C), 129.67, 130.51, 131.97, 132.37 (Ar-CH), 132.49 (Ar-C), 132.78 (Ar-CH), 134.85 (Ar-C), 137.97 (CH_2=*C*), 161.76, 162.17 (Ar-C-O), 165.09 (C=O ester), 195.58, 202.53 (C=O ketone) ppm.

^{1}H-NMR (400 MHz, $CDCl_3$, TMS): δ = 1.53 (6H, s, CH_3), 1.95 (1H, s, O-H), 4.23 (2H, t, CH_2-O), 4.51 (2H, t, CH_2-O), 4.75 (2H, t, CH_2-O), 5.98, 6.39 (2H, s, CH_2=C), 6.85-7.98 (13H, m, Ar-CH) ppm.

FTIR (ATR): 2909 (C-H), 1720 (C=O, ester), 1660 (C=O, ketone), 1147 (C-O) cm^{-1}.

3.3.3. Synthesis of PI2

The acid chloride of TBBr-BP-CA was prepared with the same procedure as in PI1. On the next step, instead of using Irgacure 2959, sesamol was used.

To a solution of the acid chloride (0.35 g, 1.072 mmol) in 2.70 mL of dry dichloromethane, sesamol (0.16 g, 1.18 mmol) was added at room temperature. Then a solution of 2.15 mL of dry dichloromethane and pyridine (0.095 mL (0.094 g), 1.18 mmol) was added in an ice bath. The reaction went on for 2.5 hours at room temperature. Once the reaction was over the solution was mixed with 30 mL of dichloromethane and was first extracted with water (3 x 9 mL) and then with NaOH (2 x 9 mL). The organic phase was dried over with sodium sulfate, filtered and the solvent was evaporated with the rotary evaporator. The remaining reddish brown solid was recrystallized from methanol and the pure product was obtained (mp 108 °C) in 30% yield.

^{13}C NMR (400 MHz, $CDCl_3$, TMS): δ = 66.05 (CH_2-O), 101.73 (O-CH_2-O), 103.59 (Ar-CH), 107.95 (Ar-CH), 113.82 (Ar-CH), 114.28 (Ar-CH), 128.15 (Ar-CH), 128.60 (*C*H_2=C), 129.68 (Ar-CH), 130.67 (Ar-C), 131.92 (Ar-CH), 132.51 (Ar-CH), 134.81 (Ar-C), 138.05 (CH_2=*C*), 144.60 (Ar-C), 145.49 (Ar-C), 148.02 (Ar-C), 161.66 (Ar-C), 163.95 (C=O, ester), 195.38 (C=O, ketone) ppm.

^{1}H-NMR (400 MHz, $CDCl_3$, TMS): δ = 4.86 (2H, s, CH_2-O), 5.83, 6.14 (2H, s, CH_2=C), 5.94 (O-CH_2-O), 6.51-7.79 (12H, m, Ar-CH) ppm.

FTIR (ATR): 2909 (C-H), 1719 (C=O, ester), 1645 (C=O, ketone), 1143 (C-O) cm^{-1}.

3.4. Synthesis of PI3

This monomer was synthesized according to a literature procedure [60].

3.4.1. Synthesis of 2-hydroxy-thioxanthone

Thiosalicylic acid (2.25 g, 15 mmol) was slowly added to 22.5 mL of concentrated H_2SO_4 and the mixture was stirred for 10 minutes. Phenol (7.05 g, 75 mmol) was then added slowly to the stirred mixture over a period of 10 minutes. Once the addition of phenol was over, the reaction mixture was further stirred at R.T for 1 hour and then at 70 °C for 4 hours. At the end of this period, it was left to stand at R.T overnight. The resulting mixture was precipitated in a large scale of boiling water and then recrystallized from 70% dioxane and 30% H_2O.

3.4.2. Synthesis of TBBr-TX

To a mixture of 2-hydroxythioxanthone (1.13 g, 4.96 mmol) and K_2CO_3 (7.11 g, 51.46 mmol) in acetone (10 mL) under nitrogen, TBBr (1.18 g, 5.32 mmol) was added dropwise at room temperature. After stirring at 60 °C for 48 h, the solvent was removed under reduced pressure. Dichloromethane (5 mL) was added and the solution was extracted with water (3 x 5 mL). And then, the organic phase was extracted with %1 NaOH (2 x 2 mL) to remove phenol. The organic phase was dried over anhydrous sodium sulfate, filtered and the solvent was evaporated under reduced pressure. The residue was purified by recrystallization from methanol to give the pure product as a yellow-orange solid in 53% yield (mp 106-107 °C).

^{13}C NMR ($CDCl_3$, 400 MHz, δ): 27.35 (CH_3), 65.86 (CH_2-O-Ar), 80.72 (C-O), 110.79 (Ar-CH), 121.70 (Ar-CH), 124.69 (*C*H_2=C), 124.88 (Ar-CH), 125.05 (Ar-CH), 126.26 (Ar-C), 127.51 (Ar-C), 128.38 (Ar-CH), 128.81 (Ar-C), 129.12 (Ar-CH), 130.95 (Ar-CH), 136.00 (Ar-C), 136.35 (*C*=CH_2), 156.14 (Ar-C), 163.44 (C=O ester), 178.53 (C=O ketone) ppm.

^{1}H-NMR ($CDCl_3$, 400 MHz, δ): 1.46 (s, 9H, CH_3), 4.78 (s, 2H, CH_2-O), 5.86 (s, 1H, CH_2=C), 6.27 (s, 1H, CH_2=C), 7.23 (s, 1H, Ar-CH), 7.25 (s, 1H, Ar-CH), 7.43 (t, 2H, Ar-CH), 7.52 (d, 1H, Ar-CH), 8.06 (s, 1H, Ar-CH), 8.56 (d, 1H, Ar-CH) ppm.

FTIR(ATR, cm^{-1}): 2974 (C-H), 1707 (C=O ester), 1633 (C=O ketone), 1145 (C-O) cm^{-1}.

3.4.3. Synthesis of TBBr-TX-CA

TFA (0.36 mL, 4.75 mmol) was added dropwise to TBBr-TX (0.5 g, 1.36 mmol) in an ice bath under nitrogen. The mixture was stirred at room temperature for 24 h. After removal of excess TFA, the crude product was recrystallized from methanol to give the pure product as a yellow solid in 50-60 % yield. Melting point could not be detected due to degradation of the sample.

^{13}C NMR (DMSO, 400 MHz, δ): 66.42 (CH_2-O-Ar), 109.51 (Ar-CH), 111.51 (Ar-CH), 122.79 (Ar-CH), 126.53 (Ar-CH), 126.60 (*C*H_2=C), 126.70 (Ar-C), 127.68 (Ar-C), 128.19 (Ar-CH), 128.61 (Ar-C), 129.06 (Ar-CH), 129.42 (Ar-CH), 132.78 (Ar-C), 136.73 (*C*=CH_2), 156.85 (Ar-C), 166.42 (C=O acid), 178.40 (C=O ketone) ppm.

^{1}H-NMR (DMSO, 400 MHz, δ): 4.36 (s, 2H, CH_2-O), 5.99 (s, 1H, CH_2=C), 6.30 (s, 1H, CH_2=C), 7.17 (d, 1H, Ar-CH), 7.57 (t, 1H, Ar-CH), 7.78 (m, 3H, Ar-CH), 7.93 (d, 1H, Ar-CH), 8.46 (d, 1H, Ar-CH) ppm.

FTIR(ATR): 3202 (O-H), 1720(C=O ester), 1680 (C=O ketone), 1145 (C-O) cm^{-1}.

3.4.4. Synthesis of PI3

Nitrogen was purged through TBBr-TX-CA (0.50 g, 1.6 mmol) for 15 minutes. Then dry dichloromethane (1.91 mL) was added before putting the solution in an ice-bath. First the solution of oxalyl chloride (0.55 g, 4.35 mmol) in dry dichloromethane (2.80 mL) was added dropwise followed by the addition of 15 drops of the DMF solution (0.3 mL of dimethylformamide in 1.49 mL dry dichloromethane). The solution was first kept in ice bath for 0.5 hours and then was allowed to run for 3.5 hours at room temperature. The

solvent and the oxalyl chloride were evaporated and the remaining acid chloride was used in the next step.

To a solution of the acid chloride (0.53 g, 1.6 mmol) in 4.03 mL of dry dichloromethane Irgacure 2959 (0.39 g, 1.76 mmol) was added at room temperature. Then a solution of 3.52 mL of dry dicholoromethane and pyridine (0.14 g, 1.76 mmol) was added to the solution in an ice bath. The reaction went on for 2.5 hours at room temperature. Once the reaction was over the solution was mixed with 50 mL of dichloromethane and was first extracted with water (2 x 15 mL) and then with $NaHCO_3$ (2 x 15 mL). The organic phase was dried over with sodium sulfate, filtered and the solvent was evaporated with the rotary evaporator. The residue was washed with ether then, purified by recrystallization from methanol. The pure product was obtained as a light brown solid (no mp was observed).

^{13}C NMR ($CDCl_3$, 400 MHz, δ): 28.61 (CH_3), 30.90 (CH_3), 62,97 (CH_2-O), 65,88 (CH_2-O), 66.45 (CH_2-O), 75.79 (C-C=O), 111.72 (Ar-CH), 114.18 (Ar-CH), 122.85 (*C*H_2=C), 125.97 (Ar-CH), 126.15 (Ar-C), 126.27 (Ar-CH), 127.40 (Ar-CH), 127.96 (Ar-C), 128.49 (Ar-C), 129.68 (Ar-CH), 129.82 (Ar-CH), 130.18 (Ar-C), 132.11 (Ar-CH), 132.36 (Ar-CH), 135.11 (Ar-C), 137.40 (*C*=CH_2), 156.97 (Ar-C), 162.21 (Ar-C), 165.08 (C=O ester), 179.55 (C=O ketone), 202.51 (C=O ketone) ppm.

^{1}H-NMR ($CDCl_3$, 400 MHz, δ): 1.60 (s, 9H, CH_3), 4.31 (s, 2H, CH_2-O), 4.59 (s, 2H, CH_2-O), 4.88 (s, 2H, CH2-O), 6.07 (s, 1H, CH_2=C), 6.48 (s, 1H, CH_2=C), 6.92 (d, 1H, Ar-CH), 6.96 (d, 1H, Ar-CH), 7.28 (d, 1H, Ar-CH), 7.47 (d, 1H, Ar-CH), 7.49 (d, 1H, Ar-CH), 7.58 (t, 1H, Ar-CH), 7.61 (d, 1H, Ar-CH), 8.01 (d, 1H, Ar-CH), 8.04 (d, 1H, Ar-CH), 8.09 (d, 1H, Ar-CH), 8.6 (d, 1H, Ar-CH) ppm.

FTIR (ATR): 2927 (C-H), 1708 (C=O ester), 1644 (C=O ketone), 1620 (C=O ketone), 1155 (C-O), 3409 (O-H) cm^{-1}.

3.5. Synthesis of Polymeric Photoinitiators

The copolymerizations of PI1 were carried out in THF at 60 ^{0}C using AIBN as thermal initiator with standard freeze-evacuate-thaw procedures. For the copolymerization of PI2 and PI3 chloroform was used as a solvent. All polymers were purified by precipitation in excess amount of methanol. The pure solids were filtered, dried under vacuum and were kept in dark.

3.6. Photoinitiating Activity Measurements

Real-time infrared spectroscopy (RT-FTIR) was recorded on a Nicolet 6700 instrument (Nicolet Instrument, Thermo Company, USA) in order to demonstrate the photopolymerization kinetics of the newly synthesized photoinitiators. Under nitrogen with a mercury lamp (Omnicure s1000 – 100 W) HDDA samples were polymerized by

- PI1 (1 weight %),
- PI1 (1 wt %) / DMAEM (3 wt %),
- PPI (BMA-*co*-PI1) (1 wt %),
- BP (1 wt %) / DMAEM (3 wt %),
- BP (1 wt %) / Irgacure 2959 (1 wt %),
- PI2 (1 wt %),
- PPI (BMA-*co*-PI2) (1 wt %),
- BP (1 wt %) / Sesamol (1 wt %),
- PPI (BMA-*co*-PI3) (1 wt %),
- TX (1 wt %) / DMAEM (1 wt %),
- TX (1 wt%) / Irgacure 2959 (1 wt%).

Degree of conversions were calculated according to the formula;

$$DC\ \% = \left(1 - \frac{Abs_{1635}^{sample}/Abs_{1718}^{sample}}{Abs_{1635}^{monomer}/Abs_{1718}^{monomer}}\right) \times 100 \qquad (3.1)$$

where the double bond conversion is calculated through the ratios of the absorbances of the C=C double bond at 1635 and the C=O ester carbonyl at 1718. The ratio of the absorbances at time *t* is always divided to the initial ratio. Using the decrease in the absorbance values of the double bond and the consistence of the one belonging to the carbonyl bond the photopolymerization activity of the initiators is measured.

4. RESULTS AND DISCUSSIONS

4.1. Synthesis and Characterization of Photoinitiators

The routes for the synthesis of the monomers PI1, PI2 and PI3 have been shown in Figure 4.1, Figure 4.2 and Figure 4.3. Syntheses involve six steps: i) synthesis of TBHMA from the reaction of *tert*-butyl acrylate and paraformaldehyde in the presence of DABCO as catalyst, ii) conversion of TBHMA to the key intermediate, TBBr, on treatment with PBr_3, iii) reaction of TBBr with 4-hydroxybenzophenone for PI1 and PI2 and with 2-hydroxy thioxanthone for PI3, iv) conversion to a carboxylic acid by cleavage of *tert*-butyl groups using TFA, v) conversion to an acid chloride by using oxalyl chloride, vi) reaction of the acid chloride with Irgacure 2959 for PI1 and PI3 and sesamol for PI2. PI1 was obtained as a yellowish oily substance after purification with column chromatography. PI2 was a white solid with a melting point of 108 °C. PI3 was a light brown solid after recrystallization from methanol. They are soluble in polar organic solvents such as methylene chloride, acetone and THF but insoluble in water and ether (Table 4.1).

Monomeric photoinitiators were copolymerized with BMA under radicalic conditions using AIBN as thermal initiator to give the corresponding polymeric photoinitiators, PPI (BMA-*co*-PI1), PPI (BMA-*co*-PI2) and PPI (BMA-*co*-PI3) (Figure 4.1, 4.2, 4.3). PPI (BMA-*co*-PI1) and PPI (BMA-*co*-PI2) were prepared in two different ratios (88:12 and 75:25 mol% feed ratios, BMA:PI1 and BMA:PI2). PPI (BMA-*co*-PI3) was prepared in two different ratios as well (91:9 and 88:12 mol% feed ratios, BMA:PI3). Data concerning synthesis and properties of the polymers are reported in Table 4.2. The solubility of the polymeric photoinitiators in selected solvents are given in Table 4.1. The synthesized PPIs have good compatibility with commercial acrylate monomers such as HDDA and TMPTA.

The number average molecular weights (M_n) and polydispersity index (PDI) of the polymers are given in the last column of Table 4.2. The M_n values of the copolymers were found to be similar, in the range of 23400 - 42200.

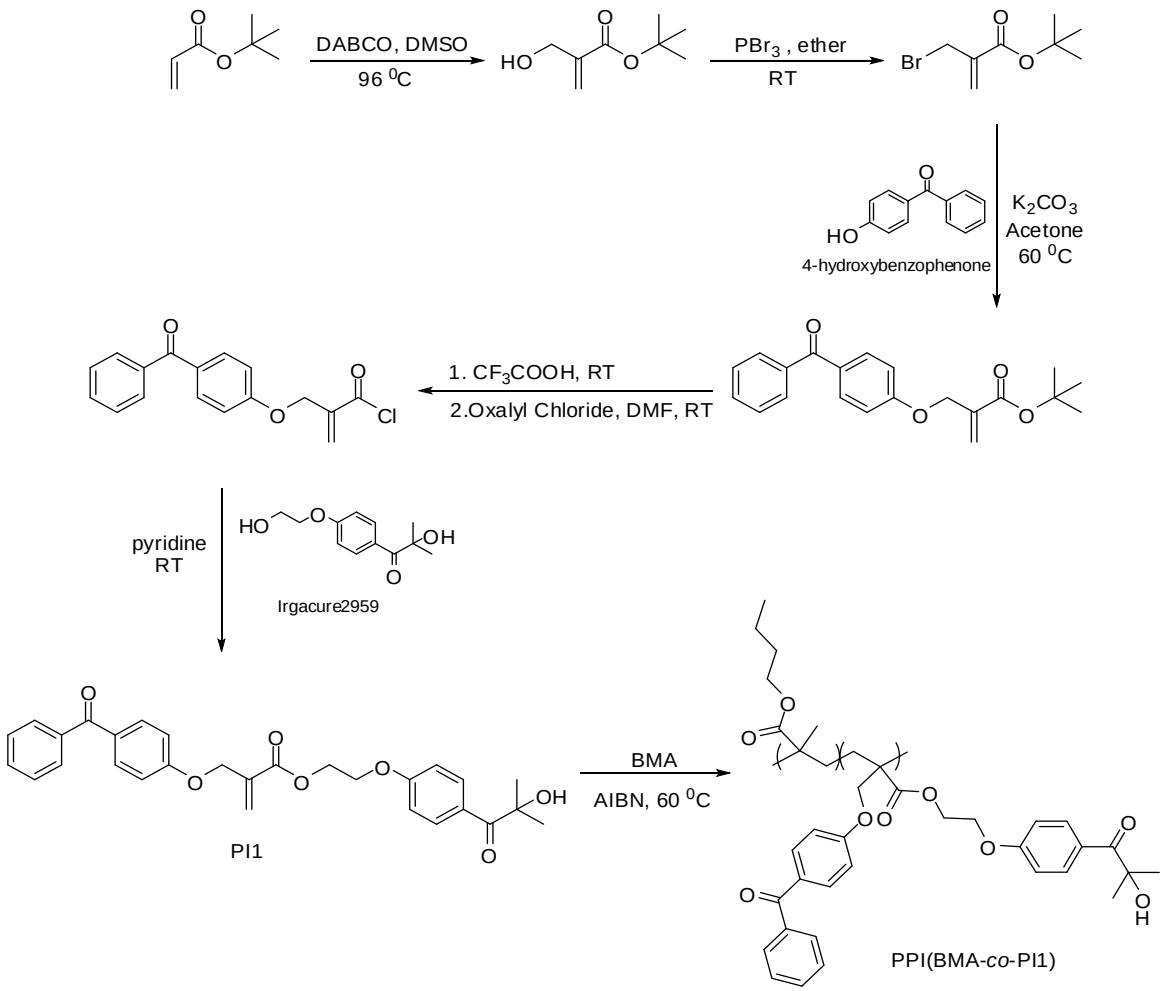

Figure 4.1. Synthesis of PI1 and its copolymers with BMA.

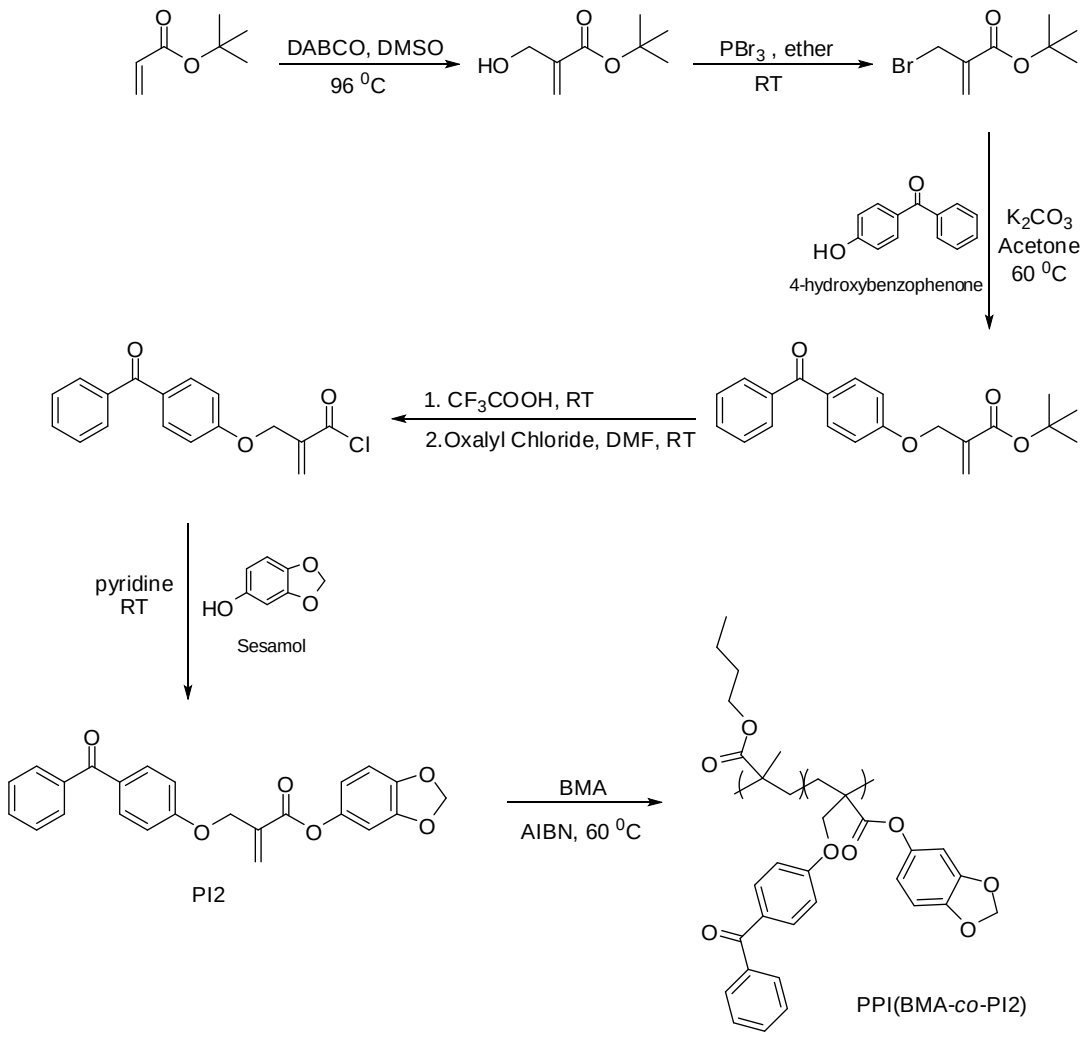

Figure 4.2. Synthesis of PI2 and its copolymers with BMA.

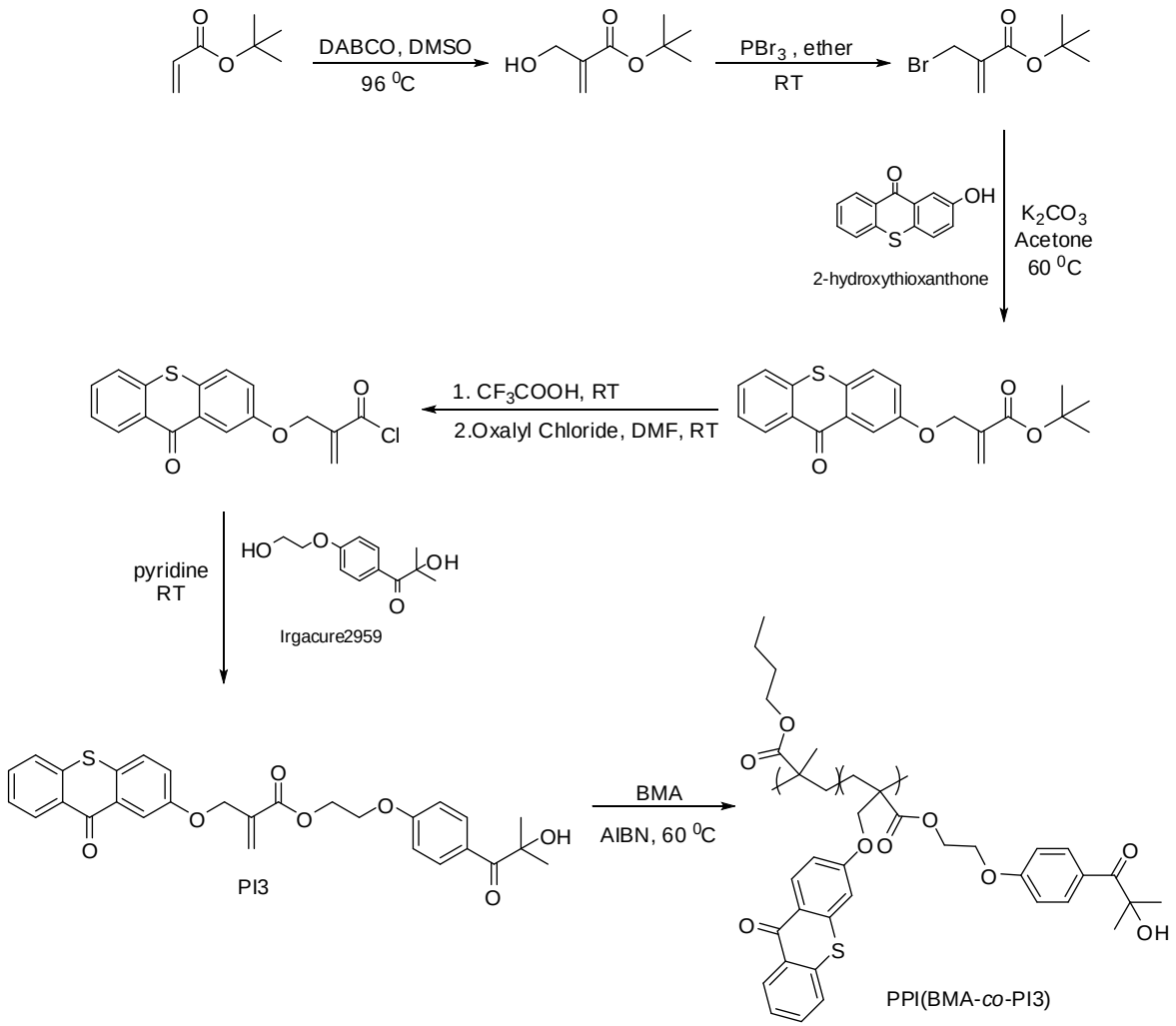

Figure 4.3. Synthesis of PI3 and its copolymerization with BMA.

Table 4.1. Solubilities of the synthesized photoinitiators in selected solvents.

Monomer / Polymer	Ether	H_2O	DCM	THF	Methanol
PI1	-	-	+	+	+
PPI (BMA-*co*-PI1)	-	-	+	+	-
PI2	-	-	+	+	-
PPI (BMA-*co*-PI2)	-	-	+	+	-
PI3	-	-	+	+	+
PPI (BMA-*co*-PI3)	+	-	+	+	-

Table 4.2. Synthesis and characterization data for polymeric photoinitiators.

Polymer	PI in feed (mol %)	PI in copolymer (mol%)	[AIBN] $x10^{-2}$	Time (h)	Yield (%)	T_g (°C)	M_n/PDI
BMA-*co*-PI1	12	7	1.8	4.5	29	-	-
BMA-*co*-PI1	12	4	1.8	22	37	37	32440/2.7
BMA-*co*-PI1	12	7	3.5	3.5	38	47	-
BMA-*co*-PI1	12	4	1.8	7.5	24	-	37230/1.86
BMA-*co*-PI1	25	13	3.5	3	35	51	-
BMA-*co*-PI2	12	17	1.8	23	45	-	23420/2.0
BMA-*co*-PI2	12	-	1.8	18	24	-	-
BMA-*co*-PI2	12	25	1.8	18	29	74	-
BMA-*co*-PI2	25	25	1.8	18	36	-	-
BMA-*co*-PI3	9	4	1.8	4	45	36	42220/3.2
BMA-*co*-PI3	12	11	1.8	3.5	31	53	-

IR and NMR spectra of the synthesized PIs were examined and found in full agreement with the proposed structures. For example, ^{1}H NMR spectrum of PI1 showed characteristic peaks for oxymethylene protons at 4.23, 4.51 and 4.75 ppm, double bond protons at 5.98 and 6.39 ppm and aromatic protons between 6.85 and 7.98 ppm (Figure 4.4). The ^{13}C NMR of PI1 showed the carbonyl peak of the ester group at 165.09 ppm and

the two carbonyl peaks of the ketone groups at 195.58 and 202.53 ppm, proving the addition of Irgacure 2959 to acid chloride intermediate bearing benzophenone as side chain (Figure 4.5).

The ^{1}H NMR spectrum of PI2 showed the characteristic peak for the methylene protons between two oxygen atoms at 5.94 ppm, the double bond protons at 5.83 and 6.14 ppm and the aromatic protons between 6.51 and 7.79 ppm (Figure 4.6). This shows that the addition of sesamol was successfully done. The ^{13}C NMR showed the peaks for the carbonyl carbon for the ketone and the ester at 195.45 and 164.02 ppm, respectively (Figure 4.7).

^{1}H NMR spectrum of PI3 also indicates two triplets at 4.31 and 4.59 ppm corresponding to methylene units of Irgacure 2959 (Figure 4.8).

IR spectra of all monomeric photoinitiators showed peaks due to both the ester and ketone C=O (Figure 4.9, 4.10, 4.11).

FTIR and ^{1}H NMR spectra of the copolymeric PPIs were also examined and the NMR spectra showed that the the double bonds of the monomers disappeared indicating that the polymerization reaction occurred successfully (Figure 4.12, Figure 4.13). Also, a slight shift has been noticed in the carbonyl peaks belonging to the ester group in the FTIR spectra of the copolymers which can be attributed to the loss of the conjugation due to the double bond (Figure 4.9, Figure 4.10, Figure 4.11). Figure 4.12 shows the ^{1}H NMR spectrum of the copolymers of PI1 with BMA. The peaks around 7-8 ppm are due to protons of the aromatic rings of BP and Irgacure 2959 which belong to PI1. The higher intensity in that area for the NMR spectrum below validates the higher composition of PI1 in that particular polymer. Copolymers' composition was determined using ^{1}H NMR, by integration of aromatic protons of PI1 with respect to oxymethylene protons of PI1 and BMA at around 4.0 ppm. (Table 4.2).

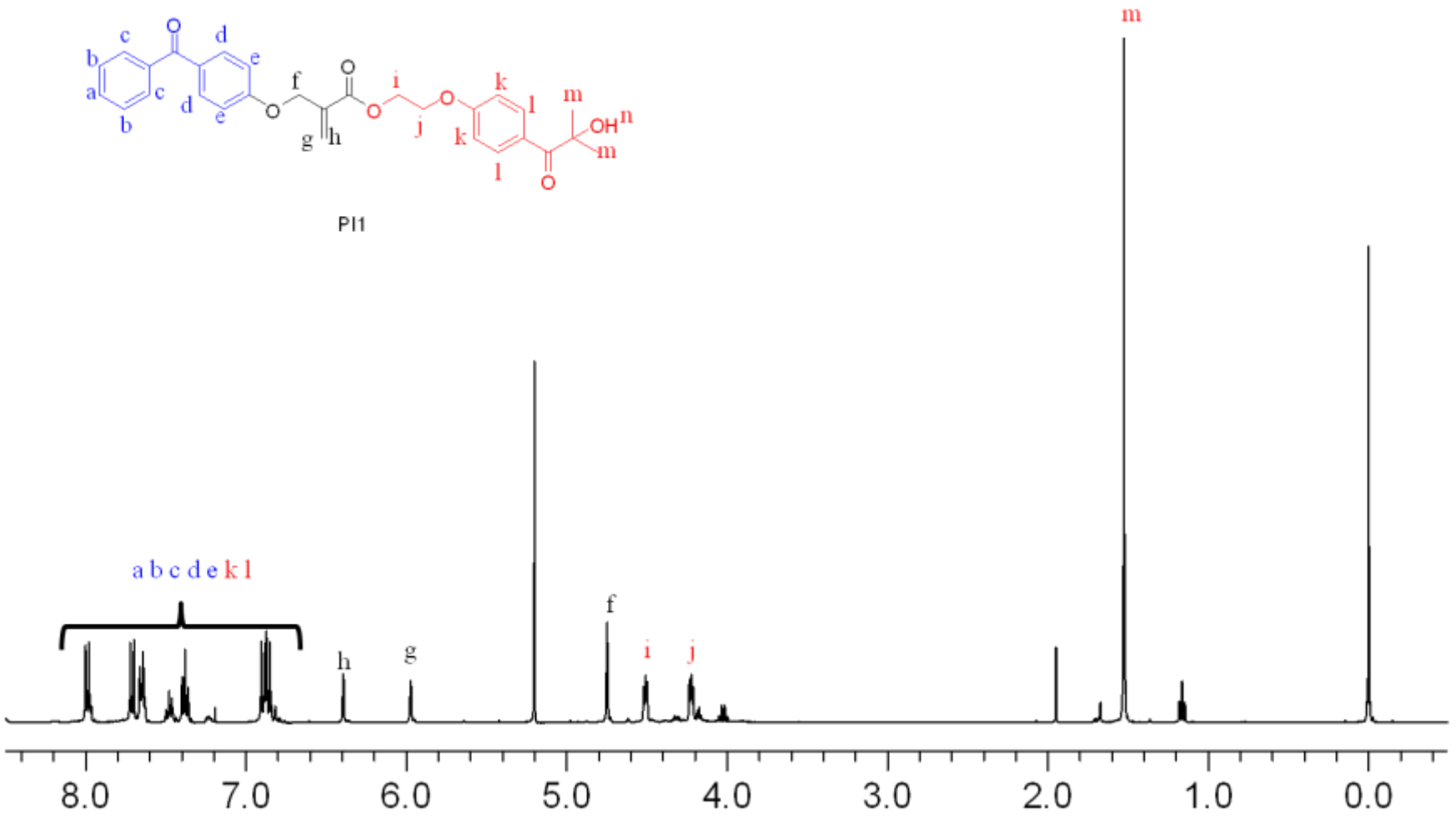

Figure 4.4. ^{1}H NMR spectrum of PI1.

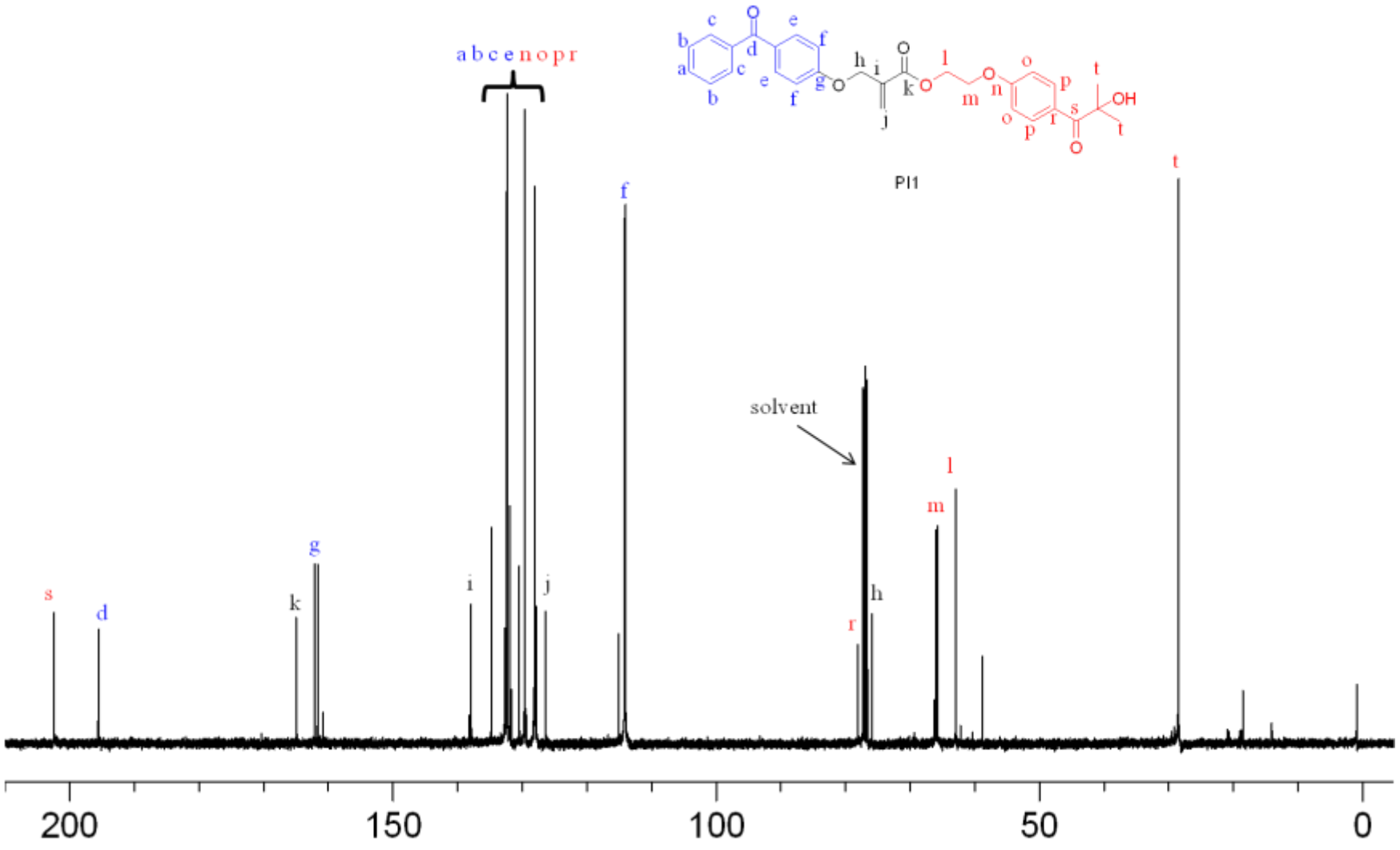

Figure 4.5. ^{13}C NMR spectrum of PI1.

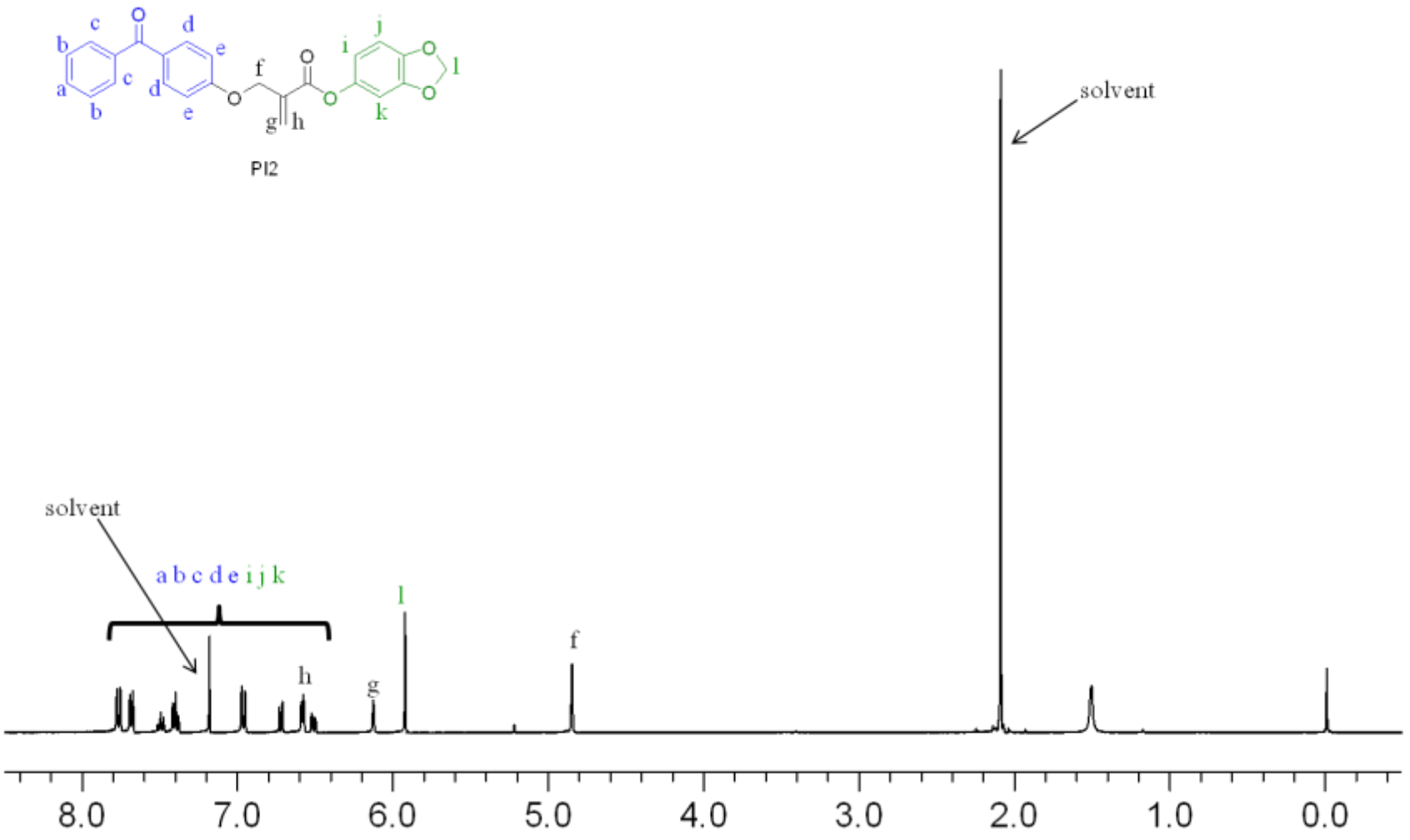

Figure 4.6. ^{1}H NMR spectrum of PI2.

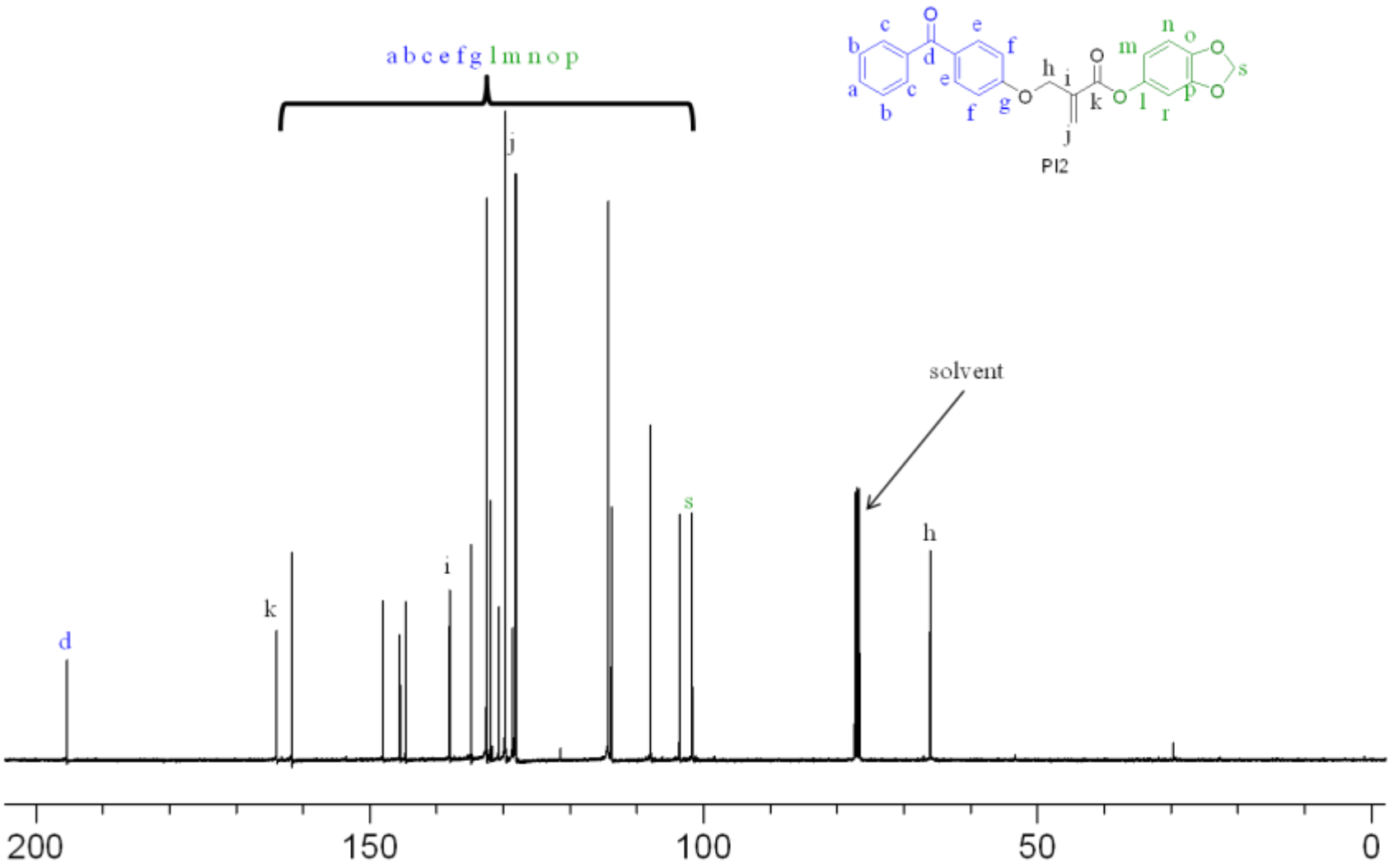

Figure 4.7. ^{13}C NMR spectrum of PI2.

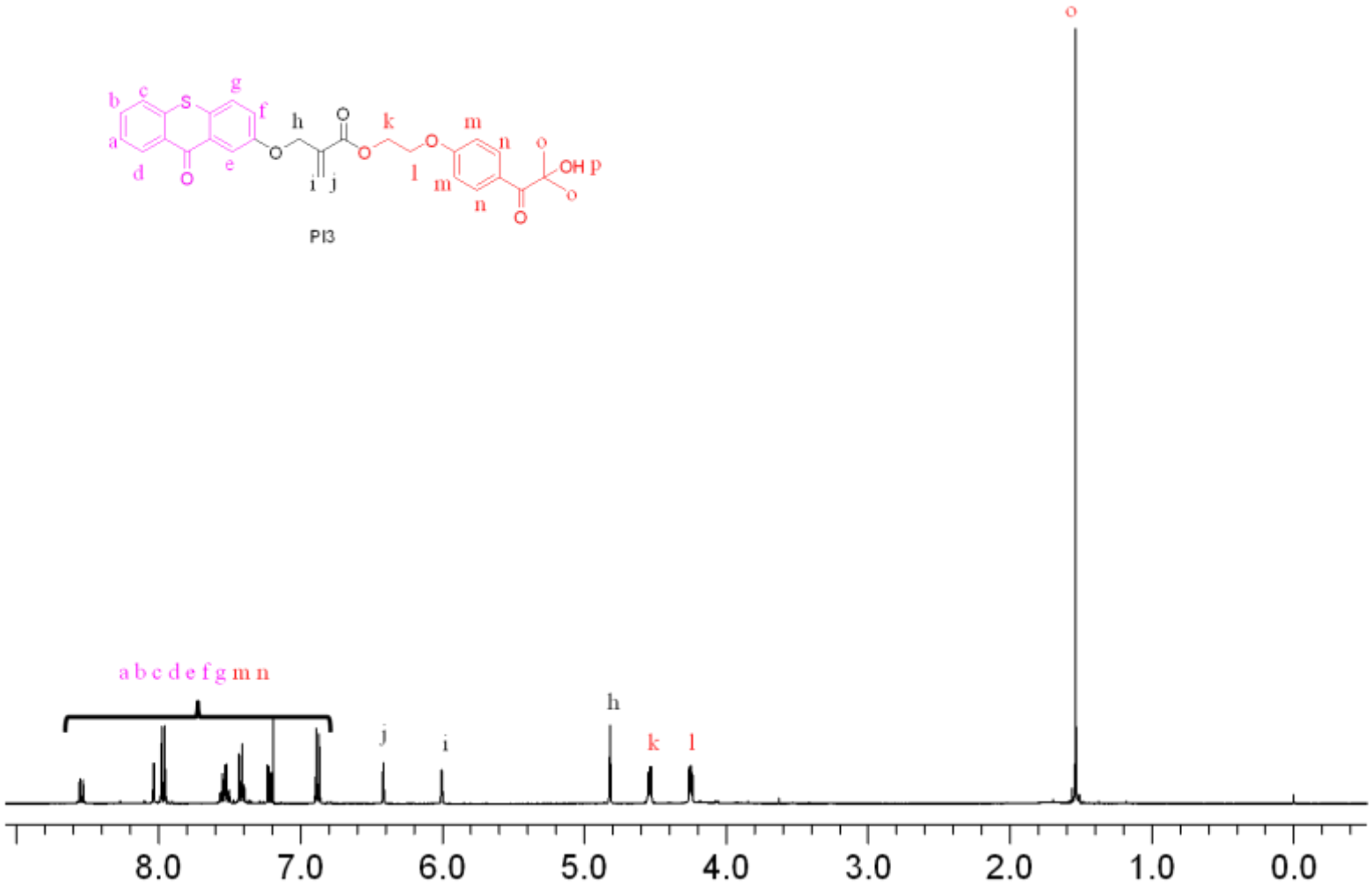

Figure 4.8. ^{1}H NMR spectrum of PI3.

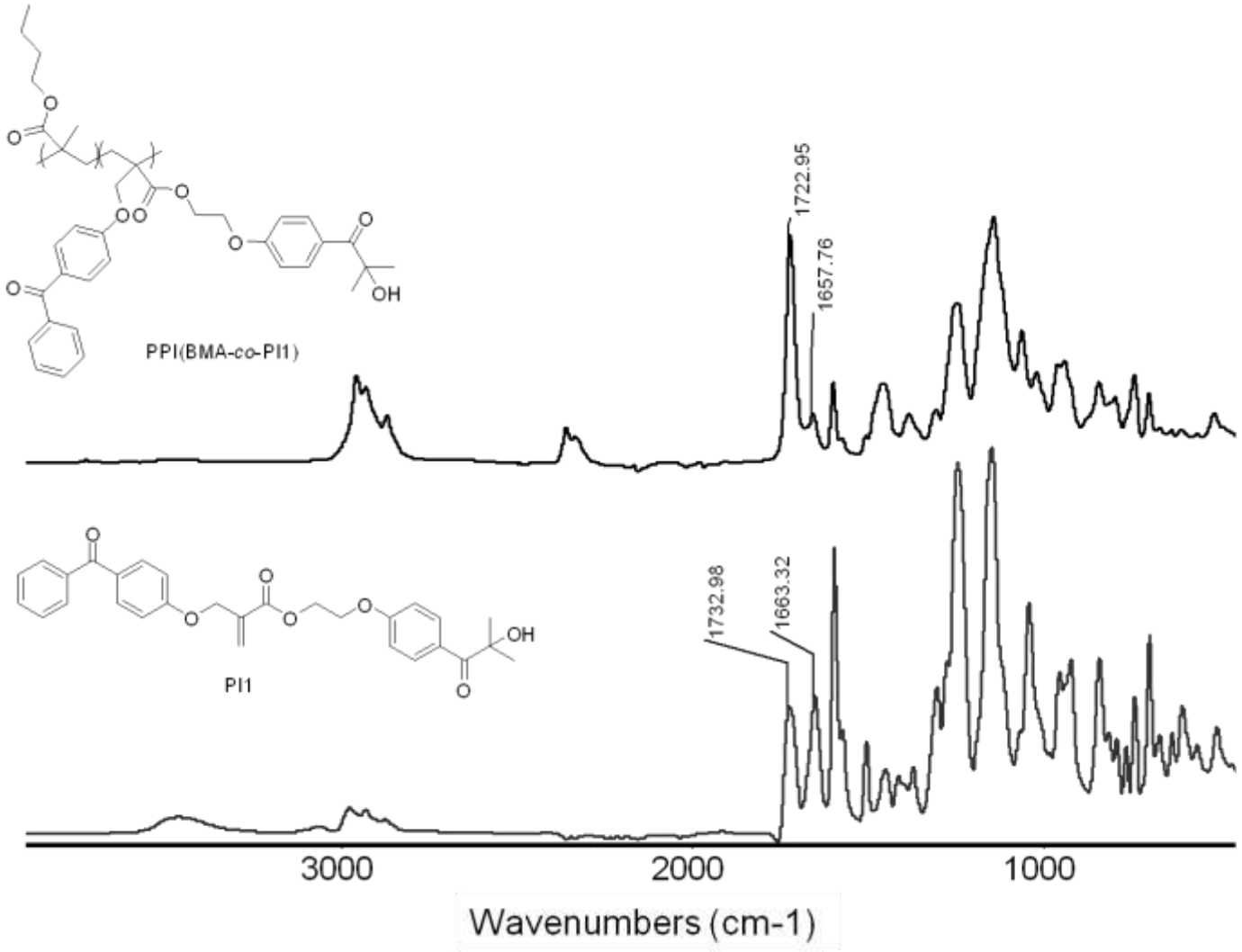

Figure 4.9. FTIR spectra of PI1 and PPI (BMA-*co*-PI1).

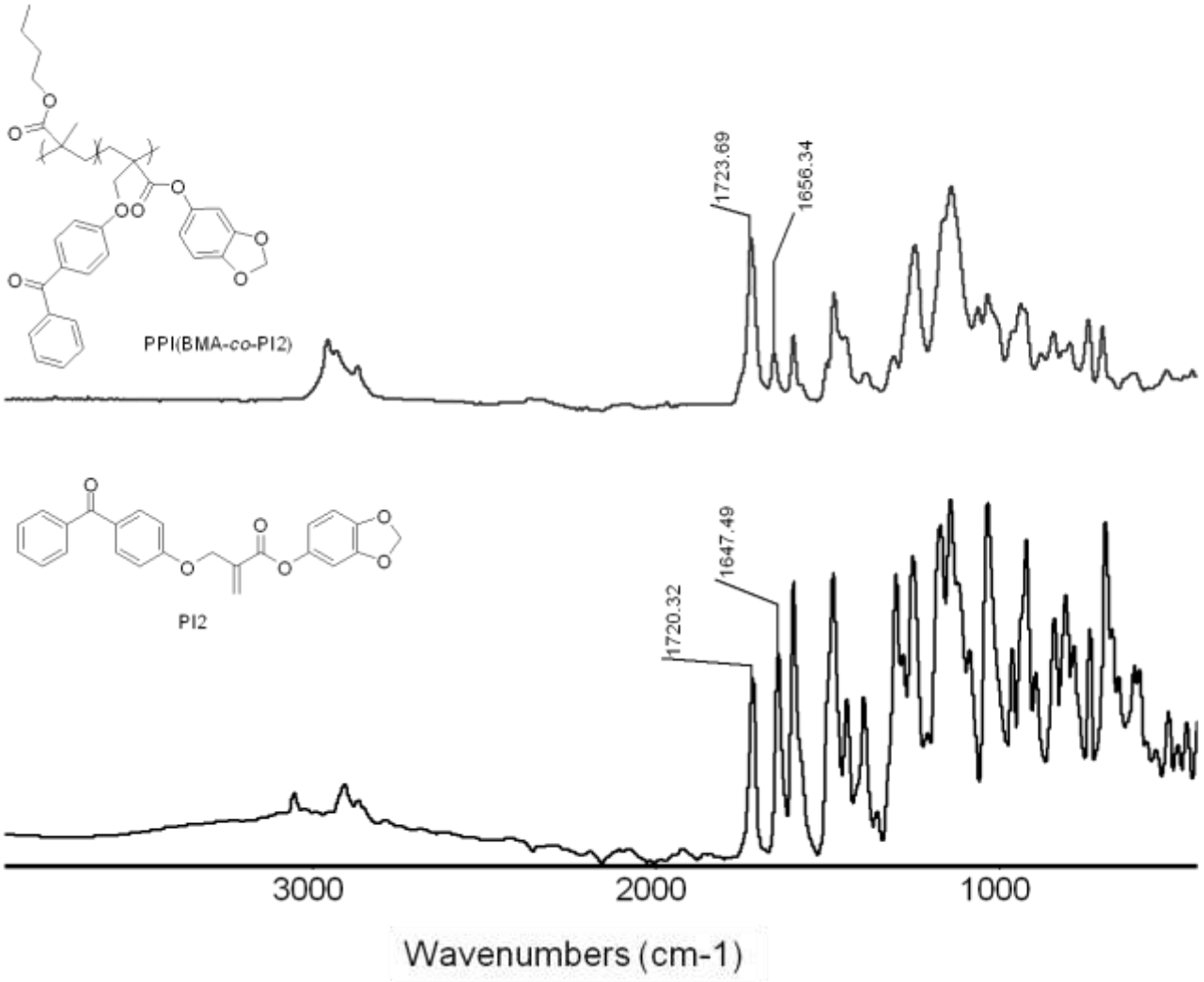

Figure 4.10. FTIR spectra of PI2 and PPI (BMA-*co*-PI2).

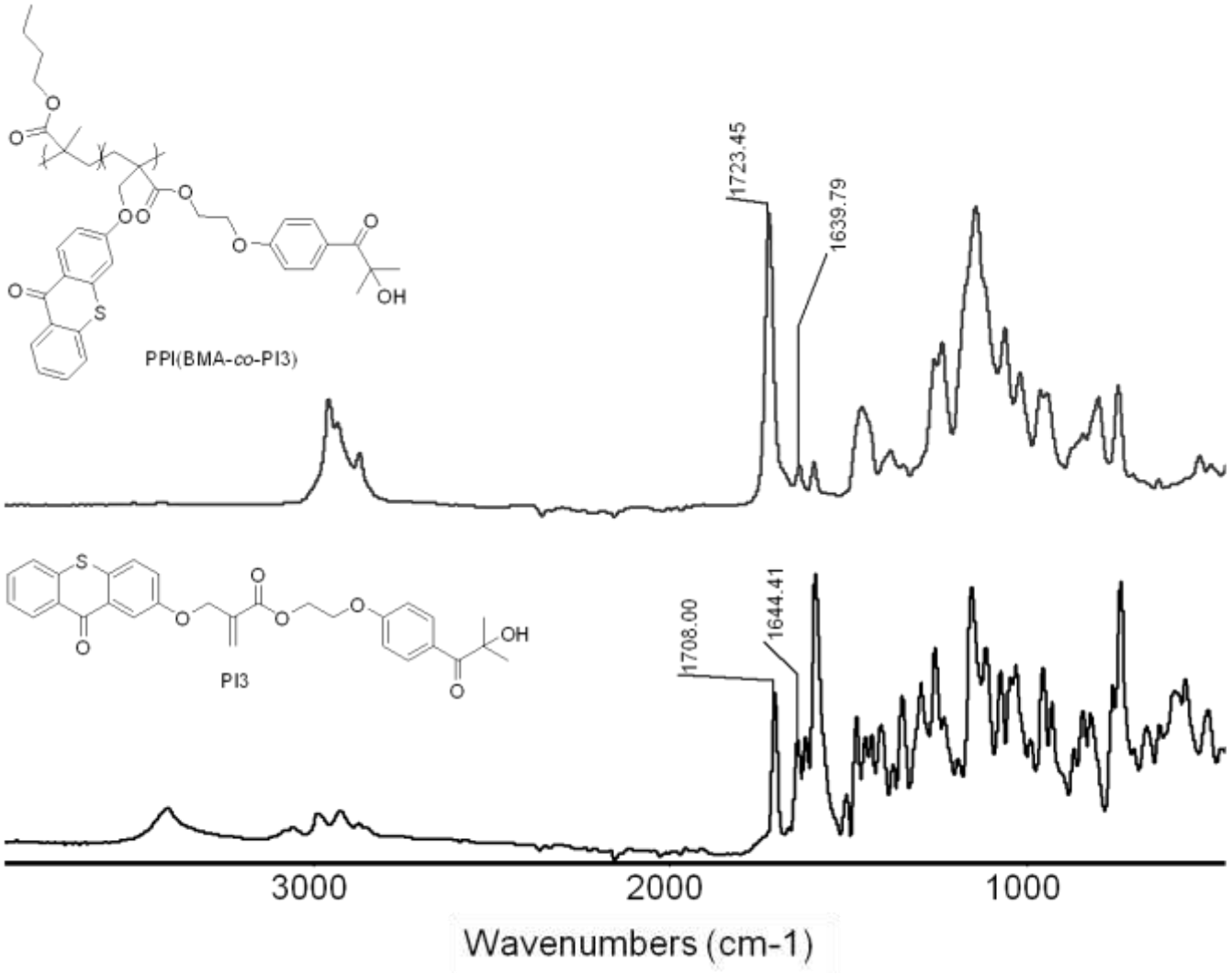

Figure 4.11. FTIR spectra of PI3 and PPI (BMA-*co*-PI3).

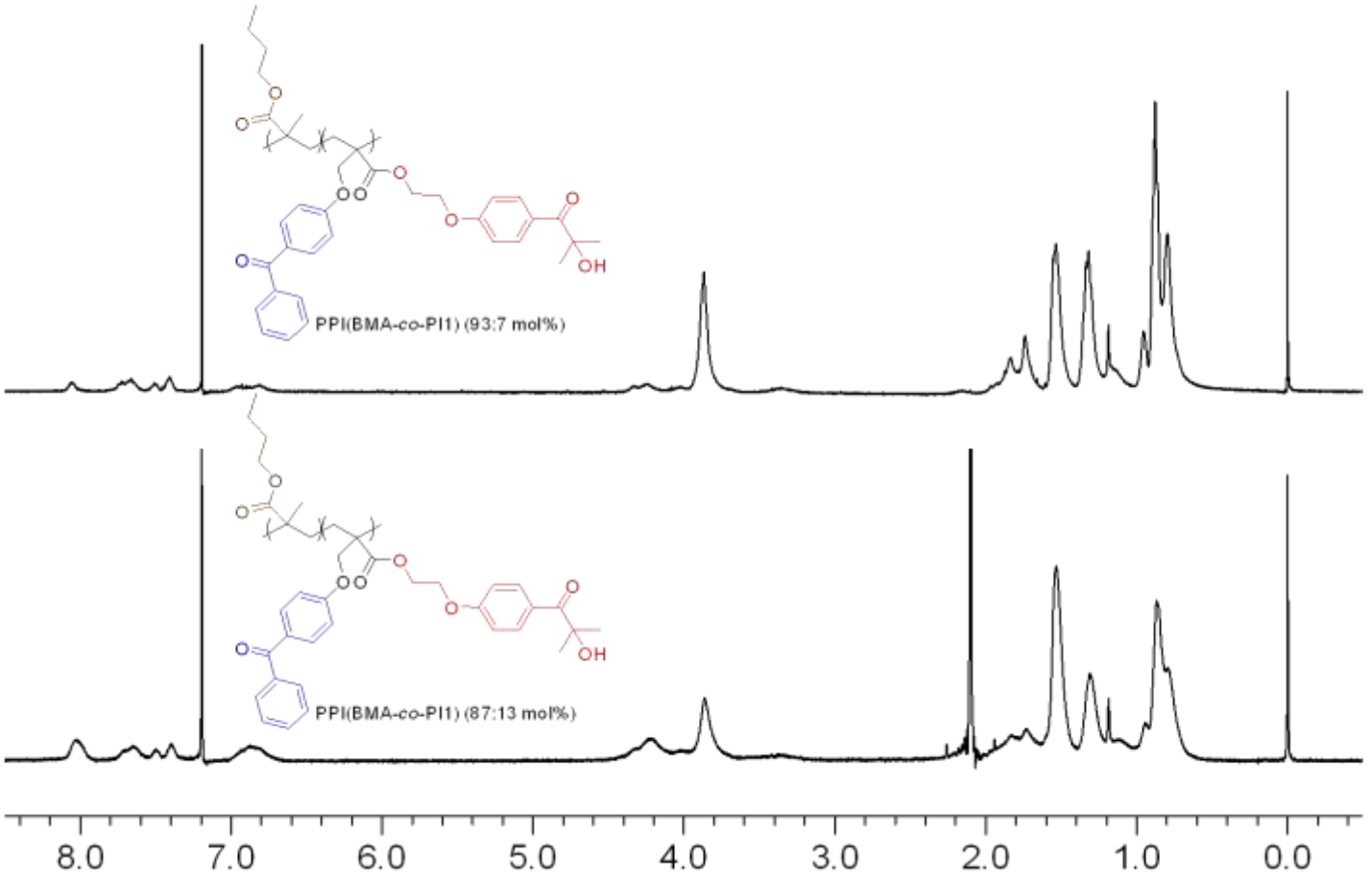

Figure 4.12. ^{1}H NMR spectra of PPI (BMA-*co*-PI1) at two different ratios.

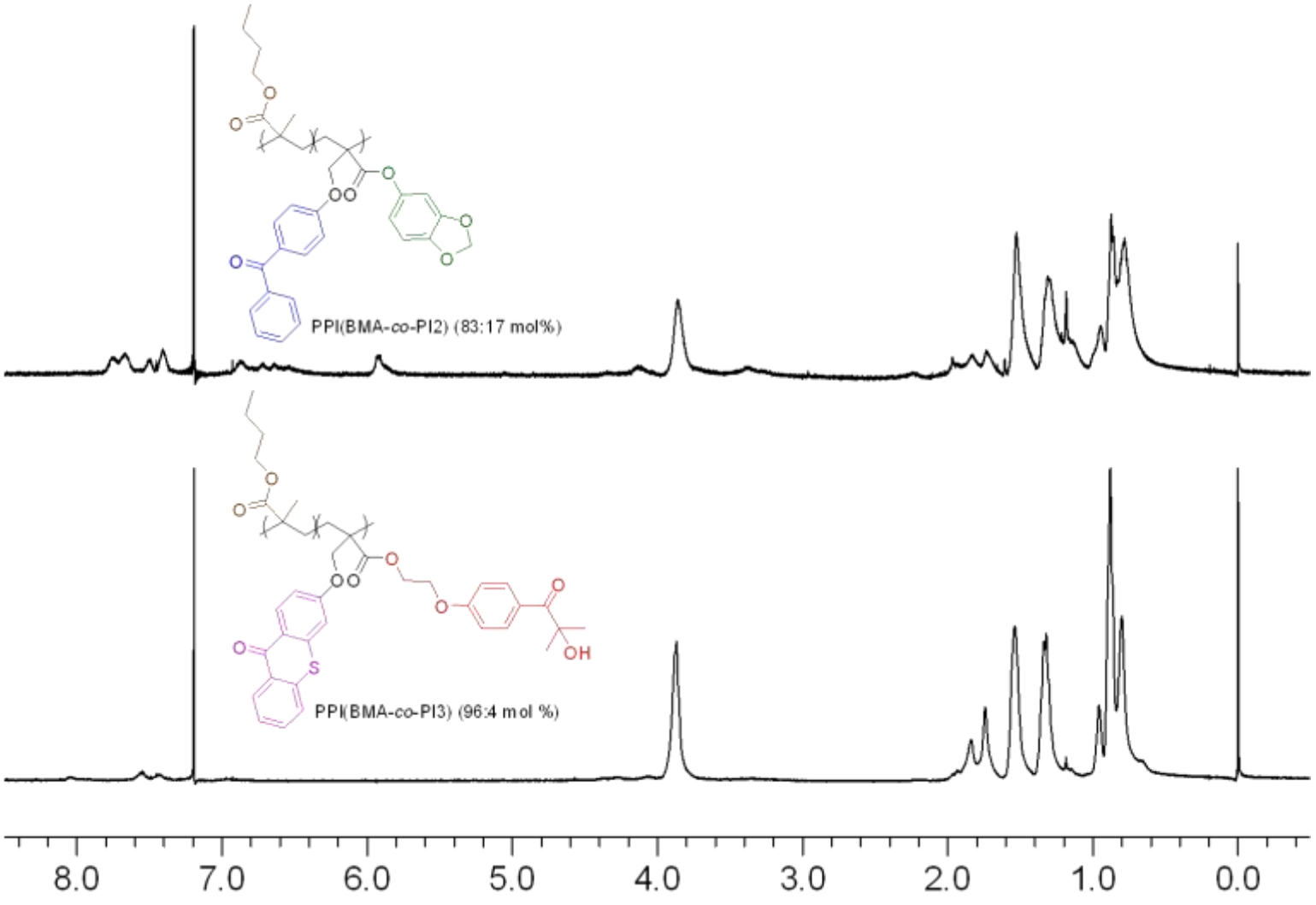

Figure 4.13. ^{1}H NMR spectra of PPI (BMA-*co*-PI2) and PPI (BMA-*co*-PI3).

The glass transition temperatures of the copolymers were measured by DSC (Table 4.2). The DSC analysis of PPI (BMA-*co*-PI1) gave different results for different copolymer compositions. For example, T_g values were found to be 37, 41 and 51 °C for the copolymers containing 4, 7 and 13% PI1 unit. As expected, PI1 with a more rigid structure increases T_g values of the copolymers. The T_g values for PPI (BMA-*co*-PI3) were found to be 36 and 53 °C for the copolymers containing 4 and 11% PI3 units. PPI (BMA-*co*-PI2) gave the highest T_g value of 73 °C (Figure 4.14).

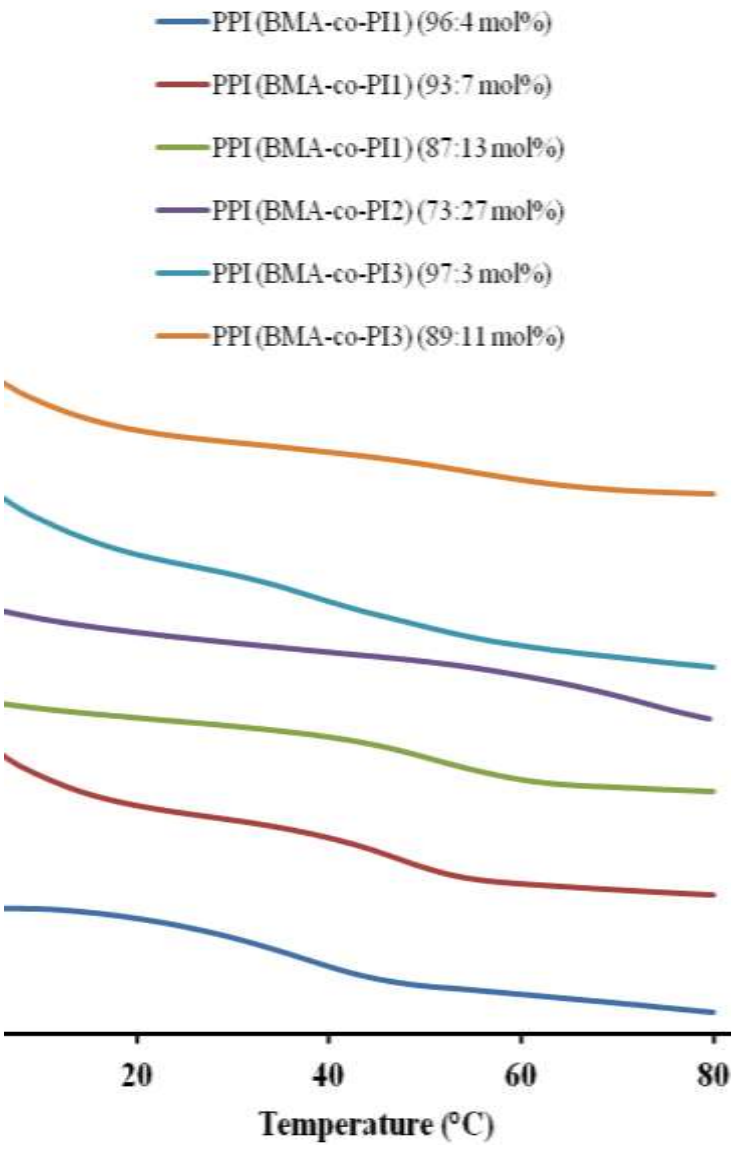

Figure 4.14. T_g analysis of polymeric photoinitiators.

4.2. UV-Vis Spectral Characterization of Photoinitiators

UV-Vis spectroscopy in chloroform was carried out to investigate the absorption characteristics of the monomeric and polymeric photoinitiators together with 4-hydroxybenzophenone, Irgacure 2959 and sesamol as references (Figure 4.15). The wavelengths for maximum absorption (λ_{max}) and the values of molar extinction coefficient at λ_{max} are given in Table 4.3.

Table 4.3. Absorption properties of the synthesized photoinitiators and their references in chloroform solution.

Photoinitiators	**λ_{max} (nm)**	**ε (M^{-1} cm^{-1})**
Irgacure 2959	278	15938
4-hydroxybenzophenone	286	17848
Sesamol	298	4238
PI1	282	30195
PI2	286	19552
PPI (BMA-*co*-PI1)	282	30171
PPI (BMA-*co*-PI2)	286	11352
PPI (BMA-*co*-PI3)	270	51067
	394	7881

4-hydroxybenzophenone, the Type II photosensitizer shows strong $\pi \rightarrow \pi^*$ absorption at 286 nm (ε = 17848). Irgacure 2959, the Type I PI gives its strong $\pi \rightarrow \pi^*$ absorption at 278 (ε = 15938). The monomeric photoinitiator PI1 that is formed by 4-hydroxybenzophenone and Irgacure 2959 shows a strong absorption at 282 nm that is slightly red-shifted compared to Irgacure 2959 with an extinction coefficient of 30195. The copolymer of PI1 with BMA also has its strong absorption at 282 nm with a similar extinction coefficient (ε = 30171) to PI1.

Sesamol is not a photoinitiator and it is solely used in the novel photoinitiator PI2 for its hydrogen donating ability, thus the low extinction coefficient at 298 nm is expected.

Therefore the monomeric photoinitiator PI2 shows a strong π → π* absorption at 286 nm (ε = 19552), the same with 4-hydroxybenzophenone. The copolymer PPI (BMA-*co*-PI2) also has a strong absorption at 286 nm though with a lower extinction coefficient (ε= 11352).

The polymeric photoinitiator PPI (BMA-*co*-PI3), having TX in its backbone, absorbs visible light (394 nm) as well as UV-light (270 nm). The strong π → π* absorption at 270 nm has an extinction coefficient of 51067, whereas the weak n → π* absorption at 394 nm has a much lower extinction coefficient of 7881. The ability of TX to absorb visible light may allow PPI (BMA-*co*-PI3) to work at visible light by transferring its triplet state energy to Irgacure 2959.

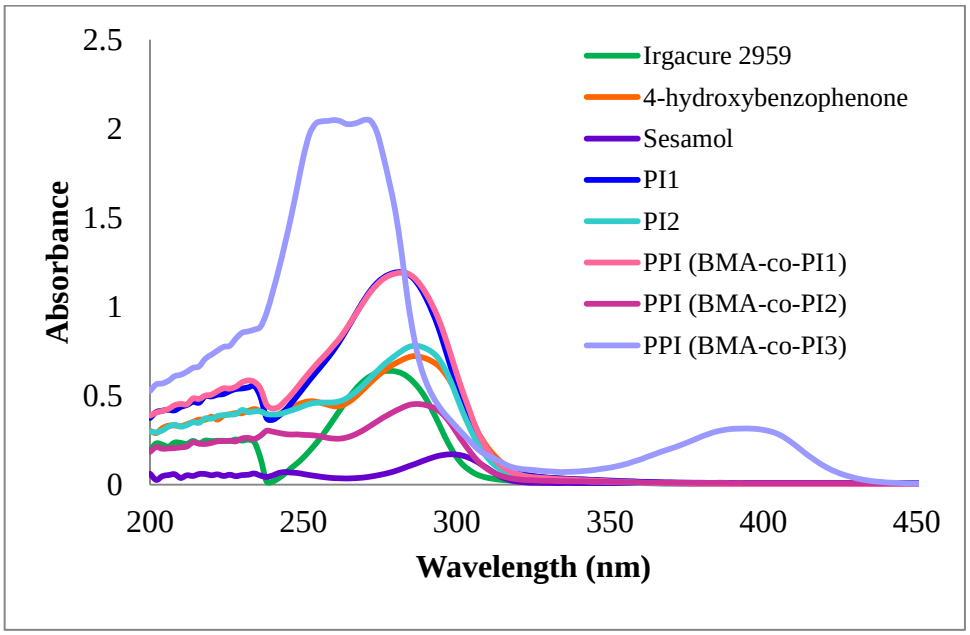

Figure 4.15. UV-Vis absorption spectra of 4-hydroxybenzophenone, Irgacure 2959, sesamol, PI1, PI2, PPI (BMA-*co*-PI1), PPI (BMA-*co*-PI2) and PPI (BMA-*co*-PI3) in chloroform (4x10-5 M) solution.

4.3. Photoinitiating Activity

The monomeric PIs (PI1 and PI2) and the polymeric PIs [PPI (BMA-*co*-PI1), PPI (BMA-*co*-PI2) and PPI (BMA-*co*-PI3)] were used to initiate photopolymerization of

HDDA and TMPTA using at 320-500 nm light under nitrogen using real-time FTIR spectroscopy. The instrument takes multiple IR spectra during the photopolymerization reaction. The conversion percentage of a monomer turning to a polymer is calculated by the ratio of the disappearance of the double bond C=C peak to the constant ester carbonyl C=O peak (eqn. 3.1). The decrease of the absorption of the double bond peak by time at 1635 cm^{-1} is clearly seen in Figure 4.16.

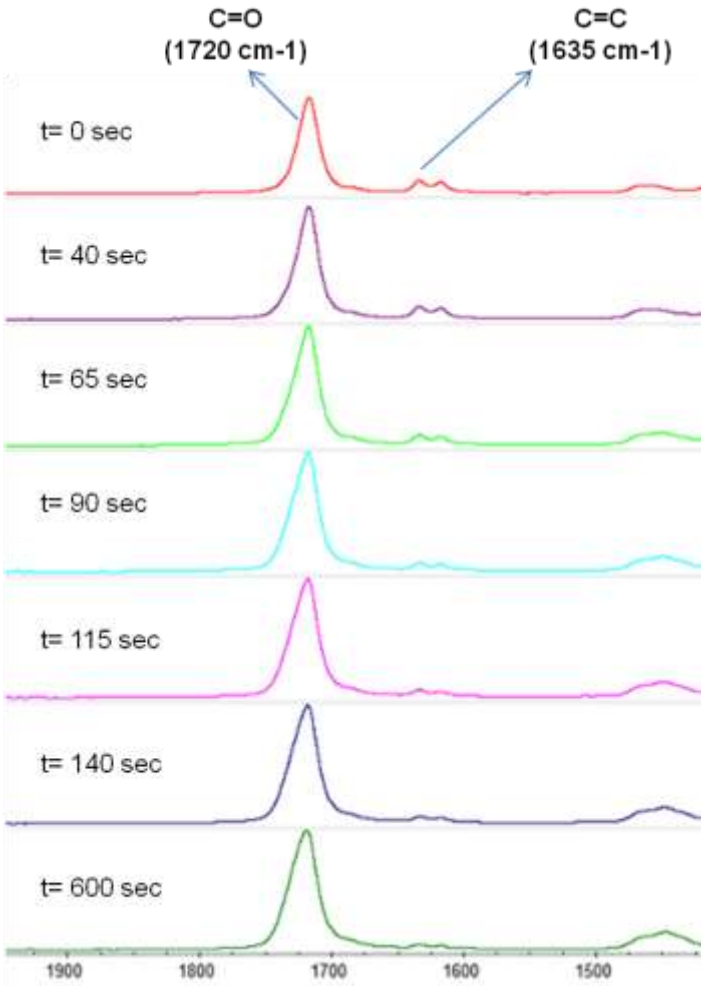

Figure 4.16. FTIR spectra of the photopolymerization reaction of HDDA by PI1 at different times.

First the photopolymerization of HDDA was performed with PI1 (1 wt%). At the used wavelength range (320-500 nm), the excitation of both chromophores of PI1 is expected. The direct excitation of Irgacure 2959 part results in radical formation by α-cleavage process. Because triplet energies of benzophenone-based PSs (E_T= 285-295

kJ/mol) are very similar to those of hydroxyalkylphenones (E_T= 280-295 kJ/mol), energy transfer may also occur from BP to Irgacure 2959 part, contributing to the α-cleavage process (Figure 4.17) [24]. Therefore BP is expected to increase the efficiency of this process. BP also acts as Type II PI, abstracting hydrogen from donors such as monomer and initiates polymerization.

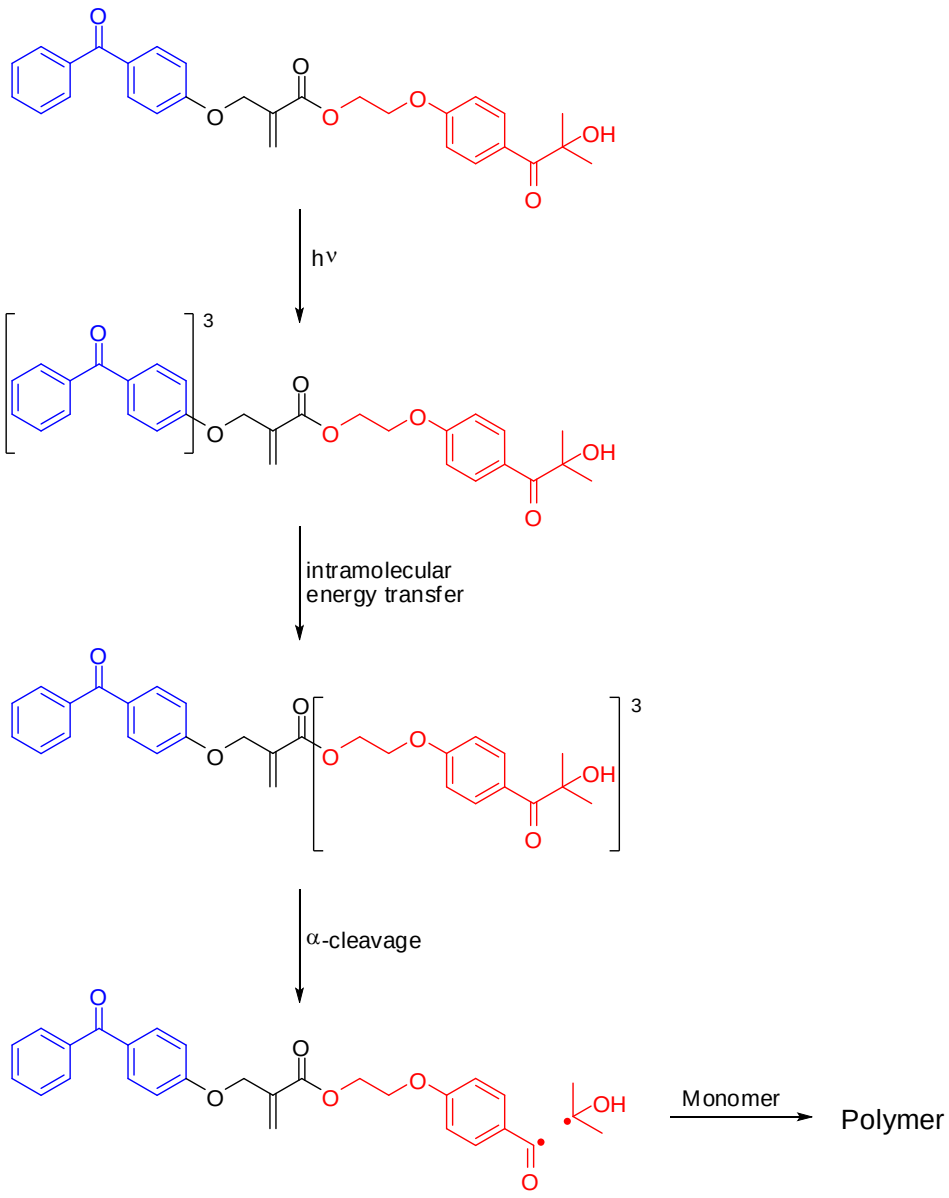

Figure 4.17. Possible photoreaction mechanism for PI1.

Figure 4.18 and Table 4.4 show the polymerization rate, conversion as well as the induction time obtained with PI1 together with PI1/DMAEM, BP/DMAEM and BP/Irgacure 2959. PI1 polymerized HDDA at a similar rate to BP/DMAEM but at a lower rate than its physical mixture (BP/Irgacure 2959). However, the conversion (66±1%) was found to be similar to those due to BP/Irgacure 2959 (74±2%) and BP/DMAEM (68±3%) mixtures. The lower rate of polymerization by PI1 than its physical mixture may indicate the absence of interaction between BP and Irgacure 2959 parts of PI1, although it is energetically favorable. Addition of the amine increased its performance by an additional Type II initiation using BP.

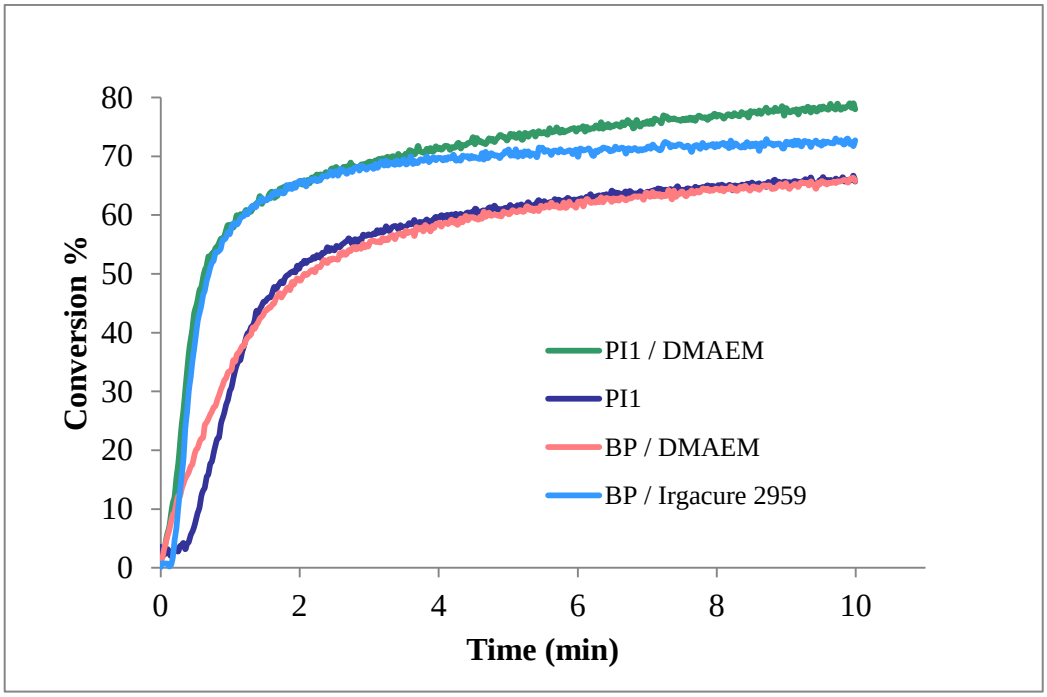

Figure 4.18. Photopolymerization profiles of HDDA initiated by PI1, PI1/DMAEM, BP/DMAEM and BP/Irgacure 2959 in nitrogen under UV light. Photoinitiator and coinitiator (DMAEM) concentrations are 1 and 3 wt% in HDDA.

Table 4.4. Conversion and induction time data for the photopolymerization of HDDA initiated by PI1, PPI (BMA-*co*-PI1) and their references in nitrogen under UV light.

Photoinitiator	Conversion (%)	t_{ind} (s)
PI1/DMAEM	77±1	12.1
PI1	66±1	24.5
PPI (BMA-*co*-PI1) (96:4 mol%)	66±1	19.9
PPI (BMA-*co*-PI1) (87:13 mol%)	69±2	1.3
BP / DMAEM	68±3	5.9
BP / Irgacure 2959	74±2	10.6

The photoinitiating activities of copolymeric photoinitiators, PPI (BMA-*co*-PI1) (96:4 mol%) and PPI (BMA-*co*-PI1) (87:13 mol%), were also investigated under the same conditions. The amount of PPIs used were 1 wt % in terms of PI1 unit in HDDA. Figure 4.19. and Table 4.4 show the conversion, the rate of the polymerization as well as the induction time. The rate of polymerization and induction time of PPI (BMA-*co*-PI1) (96:4 mol%) were found to be similar to PI1. It was observed that the rate of polymerization increases with the increase of PI1 concentration in the copolymer. Although the amount of PI is the same for both copolymers, the rate of polymerization (calculated from initial slope of conversion-time plot) of PPI (BMA-*co*-PI1) (87:13 mol%) were found to be about seven times higher than PPI (BMA-*co*-PI1) (96:4 mol%). This behavior may be due to the higher amount of polymer added in case of PPI (BMA-*co*-PI1) (96:4 mol%) which increases the viscosity of formulation and leads to lower rate of polymerizations. The t_{ind} was also higher for PPI (BMA-*co*-PI1) (96:4 mol%) for the same reason. The photoinitiating activity of PPI (BMA-*co*-PI1) (87:13 mol%) was found to be slightly higher than the BP/Irgacure 2959 mixture, confirmed by lower t_{ind} and higher rate of polymerization. The conversions reached were lower (~66-69%) for both copolymers than the BP/Irgacure 2959 (~75%) mixture.

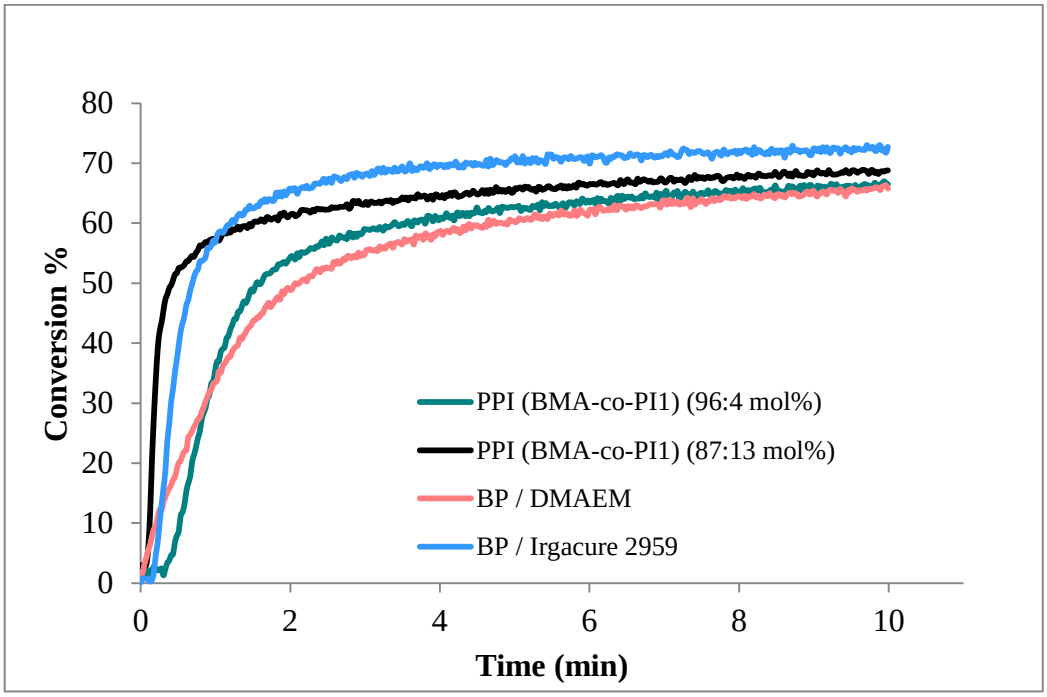

Figure 4.19. Conversion-time plots for the photopolymerization of HDDA initiated by PPIs (BMA-co-PI1), BP/DMAEM and BP/Irgacure 2959 in nitrogen under UV light. Photoinitiator and coinitiator (DMAEM) concentrations are 1 and 3 wt% in HDDA.

The photopolymerization of HDDA using the novel photoinitiator PI2 having both BP and sesamol on its side chains and its copolymers with BMA, PPI (BMA-*co*-PI2) (83:17 mol%) and PPI (BMA-*co*-PI2) (75:25 mol%), was performed (Figure 4.20 and Table 4.5). The expected photoinitiation mechanism of this initiator is shown in Figure 4.21.

Table 4.5. Conversion and induction time data for the photopolymerization of HDDA initiated by PI2 and PPI (BMA-*co*-PI2) and their references in nitrogen under UV light.

Photoinitiator	Conversion (%)	t_{ind} (s)
PI2	51±5	180.6
PPI (BMA-*co*-PI2) (83:17 mol%)	48±1	114.8
PPI (BMA-*co*-PI2) (75:25 mol%)	55±1	82.7
BP / Sesamol	64±2	4.4

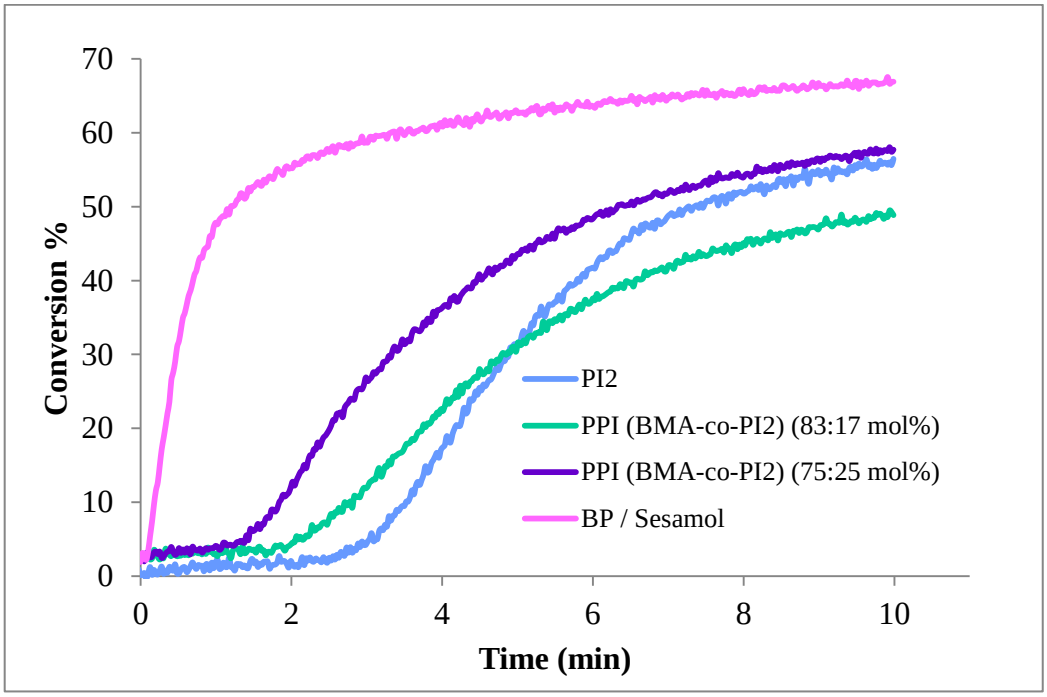

Figure 4.20. Conversion-time plots for the photopolymerization of HDDA initiated by PI2, PPI (BMA-co-PI2) and BP/Sesamol, in nitrogen under UV light. Photoinitiator and coinitiator (Sesamol) concentrations are 1 wt% in HDDA.

The initiating reactivity of PI2 was found to be much lower than its reference PI system (BP/sesamol), confirmed by very high induction time (180.6 s for PI2 vs. 4.4 s for BP/sesamol), low polymerization rate (13.9 %/s for PI2 vs 70.4 %/s for BP/sesamol) and lower conversion (51±5 % for PI2 vs 64±2 % for BP/sesamol) values.

The copolymers of PI2 with butyl methacrylate at two different compositions, PPI (BMA-*co*-PI2) (83:17 and 75:25 mol%), were used to polymerize HDDA under the same conditions. The amount of PPIs were adjusted to obtain 1 wt % PI2 in HDDA. The copolymers showed an improved t_{ind} values compared to PI2, 82.7 and 114.8 s for PPI (BMA-*co*-PI2) (75:25 mol%) and PPI (BMA-*co*-PI2) (83:17 mol%). The conversions of the copolymers were found to be similar to PI2 and lower than the reference PI (BP/sesamol). All these results indicated that PI2 and its copolymers had great potential to eliminate the conventional amine coinitiators, although the low polymerization rate may be a drawback.

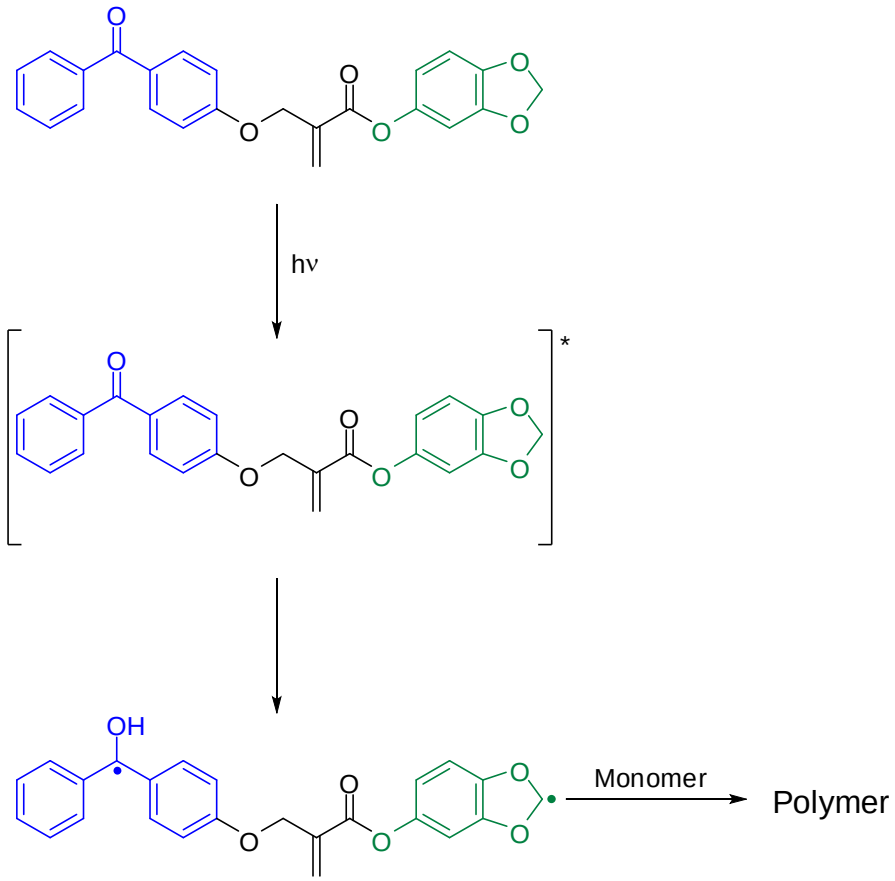

Figure 4.21. Possible photoreaction mechanism for PI2.

The copolymers of PI3 with butyl methacrylate at two different compositions, PPI (BMA-*co*-PI3) (97:3 and 89:11 mol%), were used to polymerize HDDA under the same conditions. The amount of PPIs were again used to obtain 1 wt % PI3 in HDDA. We expect excitation of both chromophores at the used wavelength range. The conversion reached for PPI (BMA-*co*-PI3) (89:11 mol%) was higher than PPI (BMA-*co*-PI3) (97:3 mol%) and comparable to TX/Irgacure 2959 system (Figure 4.22 and Table 4.6). However, t_{ind} value was significantly reduced by the use of this PI.

Because the copolymers have TX chromophore they can also be selectively excited in the visible range and transfer energy to the other chromophore. This energy may be enough for α-cleavage process and result in radical formation to initiate polymerization. To investigate their performances, selective excitation at visible range is necessary, which will be a future work.

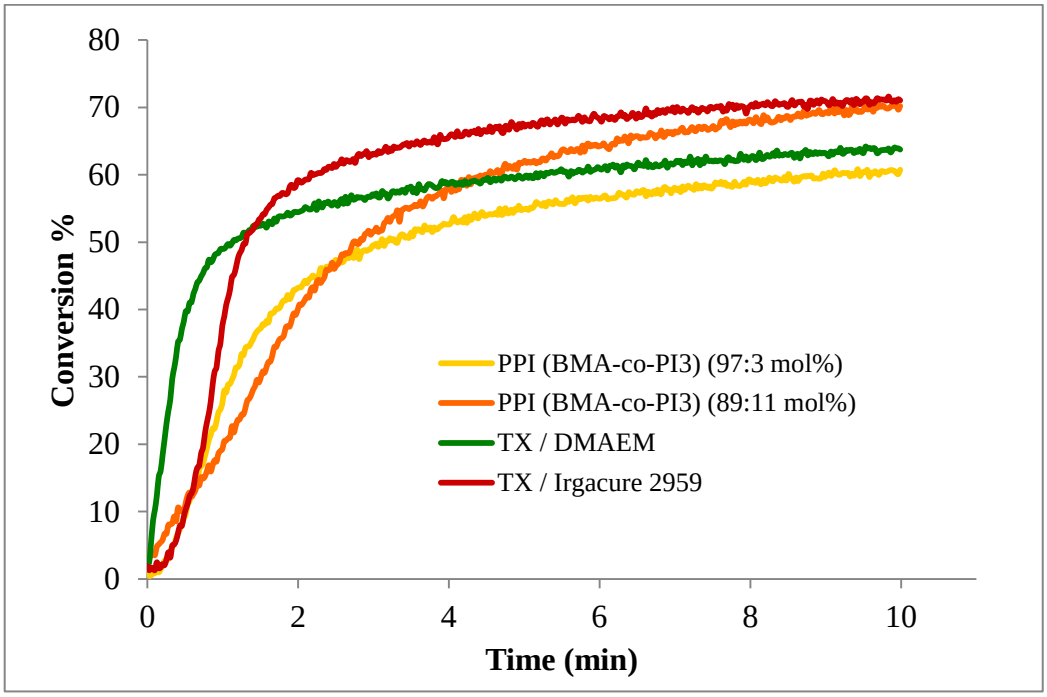

Figure 4.22. Conversion-time plots for the photopolymerization of HDDA initiated by PPIs (BMA-*co*-PI3), TX/DMAEM and TX/Irgacure 2959 in nitrogen under UV light. Photoinitiator and DMAEM concentrations are 1 wt% in HDDA.

Table 4.6. Conversion and induction time data for the photopolymerization of HDDA initiated by PPI (BMA-*co*-PI3) and their references in nitrogen under UV light.

Photoinitiator	Conversion (%)	t_{ind} (s)
PPI (BMA-*co*-PI3) (97:3 mol%)	59±1	15.1
PPI (BMA-*co*-PI3) (89:11 mol%)	70±1	1.4
TX/DMAEM	65±2	1.4
TX/Irgacure 2959	70±2	21.4

Photoinitiators PI1, PI1/DMAEM and PPI (BMA-*co*-PI1) (87:13 mol%) were used to polymerize TMPTA under the same conditions (Figure 4.23 and Table 4.7). The results were compared to those of BP/DMAEM. PI1 showed the lowest rate of polymerization and the addition of DMAEM or copolymerization with BMA increased its rate without changing the conversion. Overall conversions were similar (~33-39 %) and lower than

those obtained with HDDA systems due to higher functionality of TMPTA. However, t_{ind} values were higher for TMPTA systems due to higher viscosity of this monomer.

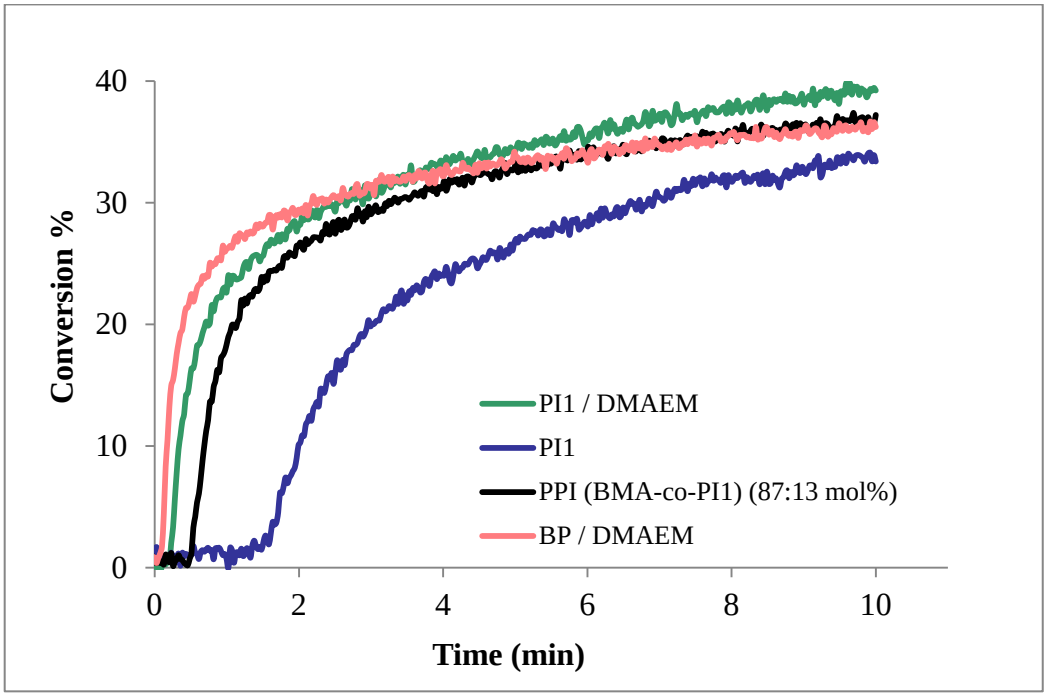

Figure 4.23. Conversion-time plots for the photopolymerization of TMPTA initiated by PI1, PI1/DMAEM, PPI (BMA-*co*-PI1) (87:13 mol%) and BP/DMAEM in nitrogen under UV light. Photoinitiator and DMAEM concentrations are 1 and 3 wt% in HDDA.

Table 4.7. Conversion and induction time data for the photopolymerization of TMPTA initiated by PI1, PI1/DMAEM, PPI (BMA-*co*-PI1) and BP/DMAEM and their references in nitrogen under UV light.

Photoinitiator	Conversion (%)	t_{ind} (s)
PI1/DMAEM	39	12.1
PI1	33	95.0
PPI (BMA-*co*-PI1) (87:13 mol%)	37	32.0
BP/DMAEM	36	7.4

Another set of experiment involved polymerization of TMPTA using PI2 under the same conditions. The reactivity of PI2, expressed by t_{ind}, conversion and the rate of polymerization, was found to be very low (Figure 4.25). Its copolymer showed an improved rate, conversion and t_{ind} values. However, its reactivity is still lower than BP/sesamol system.

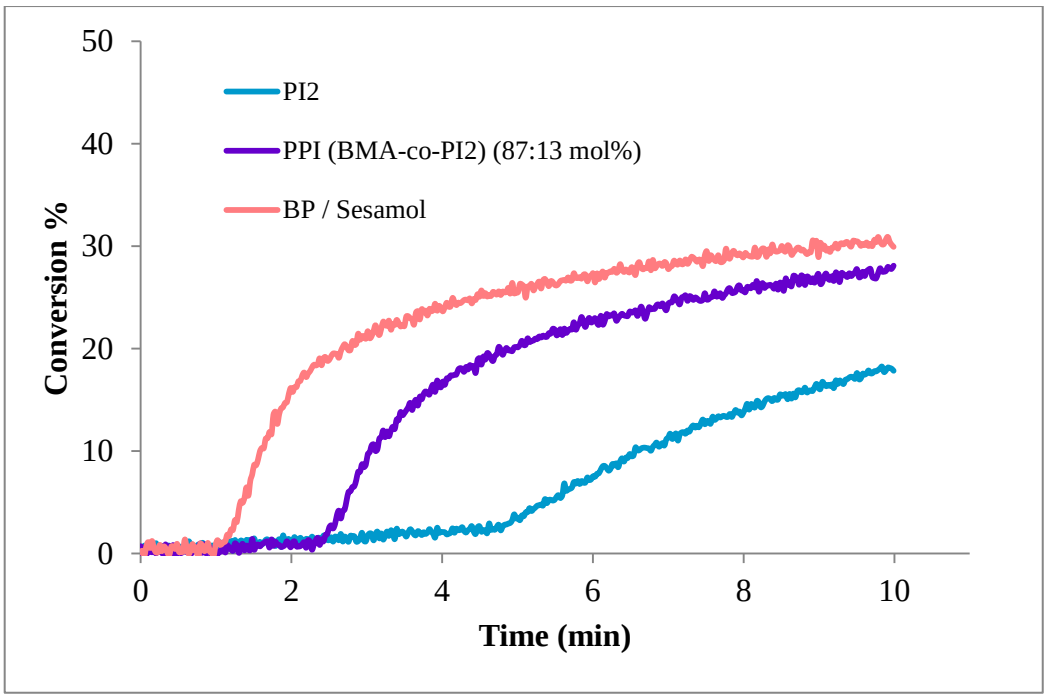

Figure 4.24. Conversion-time plots for the photopolymerization of TMPTA initiated by PI2, PPI (BMA-*co*-PI2) and BP/sesamol in nitrogen under UV light. Photoinitiator and coinitiator (Sesamol) concentrations are 1 wt% in HDDA (Copolymeric photoinitiator was used 0.69 wt% of HDDA).

Table 4.8. Conversion and induction time data for the photopolymerization of TMPTA initiated by PI2, PPI (BMA-*co*-PI2) and their references in nitrogen under UV light.

Photoinitiator	Conversion (%)	t_{ind} (s)
PI2	18	269.6
PPI (BMA-*co*-PI2) (83:17 mol%)	28	151.6
BP / Sesamol	30	67.3

5. CONCLUSION

Three monomeric photoinitiators (two of which are novel) containing i) BP and hydroxyalkylphenone- (PI1), ii) TX and hydroxyalkylphenone- (PI2) and iii) BP and sesamol were synthesized. Their copolymerization with BMA at different ratios gave new polymeric photoinitiators, PPI (BMA-*co*-PI1), PPI (BMA-*co*-PI2) and PPI (BMA-*co*-PI3).

The properties of these PI systems were investigated with UV and real-time FTIR spectroscopies. Broadband irradiation experiments for excitation of both chromophoric groups were performed for the sysnthesized PIs and for the physical mixtures of their active components.

The photoinitiating efficiency of PI1 was found to be less than the corresponding physical mixture, BP/Irgacure 2959. Among the PI1-based PIs, PPI (BMA-*co*-PI1) (87:13 mol%) was found to be most efficient, having a comparable photoinitiating reactivity with its physical mixture (BP/Irgacure 2959). The photoinitiating efficiency of PPI (BMA-*co*-PI3) (89:11 mol%) was also found to be comparable with its physical mixture. As a result, the incorporation of PI and PS in the same molecule did not increase the photoinitiation efficiency. Because there was no significant effect of sensitization under the used wavelength range (320-500 nm), experiments should be performed using specific filters.

PI2 containing both PI and coinitiator (sesamol) in its structure and its copolymers with BMA showed lower polymerization efficiencies than the BP/sesamol system. However, these PIs have great potential to eliminate amine coinitiators.

These monomeric and polymeric PIs are incorporated into the photocurable matrix, therefore they can reduce migration problems faced with small molecule nonmonomeric PIs.

REFERENCES

1. Dietliker, K., T. Jung, J. Benkhoff, H. Kura, A. Matsumoto, H. Oka, D. Hristova, G. Gescheidt and G. Rist, "New Developments in Photoinitiators", *Macromolecular Symposia,* Vol. 217, pp. 77-97, 2004.

2. Cheng, L. and W. Shi, "Synthesis and Photoinitiating Behavior of Benzophenone-Based Polymeric Photoinitiators Used for UV Curing Coatings", *Progress in Organic Coatings*, Vol. 71, pp. 355-361, 2011.

3. Yagci, Y., S. Jockush and N. J. Turro, "Photoinitiated Polymerization: Advances, Challenges, and Opportunities", *Macromolecules*, Vol. 43, pp. 6245-6260, 2010.

4. Tehfe, M. A., F. Louradour, J. Lalevée and J. P. Fouassier, "Photopolymerization Reactions: On the Way to a Green amd Sustainable Chemistry", *Applied Sciences*, Vol. 3, pp. 490-514, 2013.

5. Dietliker, K., R. Hüsler, J. L. Birbaum, S. Ilg, S. Villeneuve, K. Studer, T. Jung, J. Benkhoff, H. Kura, A. Matsumoto and H. Oka, "Advancements in Photoinitiators-Opening Up New Applications for Radiation Curing", *Progress in Organic Coatings*, Vol. 58, pp. 146-157, 2007.

6. Fouassier, J. P. and J. Lalevée, *Photoinitiators for Polymer Synthesis: Scope, Reactivity and Efficiency*, First Edition, Wiley-VCH Verlag GmbH & Co. KGaA, Weinheim, 2012.

7. Andrzejewska E., "Photopolymerization Kinetics of Multifunctional Monomers", *Progress in Polymer Science,* Vol. 26, pp. 605-665, 2001.

8. Flory, P. J., *Principles of Polymer Chemistry*, Cornell University Press, Ithaca, 1953.

9. Odian, G., *Principles of Polymerization*, Wiley-Interscience Press, New York, 1981.

10. Jenkins A. D., P. Kratochvil, R. F. T. Stepto and U. W. Suter, "Glossary of Basic Terms in Polymer Science", *Pure and Applied Chemistry*, Vol. 68, pp 2287-2311, 1996.

11. Kim, S. K. and C. A. Guyman, "Effects of Polymerizable Organoclays on Oxygen Inhibition of Acrylate and Thiol-Acrylate Photopolymerizable", *Polymer*, Vol. 53, pp. 1640-1650, 2012.

12. Kilambi, H., E. R. Beckel, K. A. Berchtold, J. W. Stansbury and C. N. Bowman, "Influence of Molecular Dipole on Monoacrylate Monomer Reactivity", *Polymer*, Vol. 46, pp. 4735-4742, 2005.

13. Decker, C. and A. D. Jenkins, "Kinetic Approach of O_2 Inhibition in Ultraviolet- and Laser-Induced Polymerizations", *Macromolecules*, Vol. 18, pp. 1241-1244, 1985.

14. Anseth, K. S., C. N. Bowman and N. A. Peppas, "Polymerization Kinetics and Volume Relaxation Behavior of Photopolymerized Multifunctional Monomers Producing Highly Crosslinked Networks", *Journal of Polymer Science: Part A: Polymer Chemistry*, Vol. 32, pp. 139-1447, 1994.

15. Young, J. S., A. R. Kannurpatti and C. N. Bowman, "Effect of Comonomer Concentration and Functionality on Photopolymerization Rates, Mechanical Properties and Heterogeneity of the Polymer", *Macromolecular Chemistry and Physics*, Vol. 199, pp. 1043-1049, 1998.

16. Fouassier, J. P., *Photoinitiation, Photopolymerization, and Photocuring: Fundamentals and Applications*, Hanser, Munich, pp. 247-254, 1995.

17. Fouassier, J. P. and J. Lalevée, *Photoinitiators for Polymer Synthesis: Scope, Reactivity and Efficiency*, First Edition, Wiley-VCH Verlag GmbH & Co. KGaA, Weinheim, pp. 11-19, 2012.

18. Fouassier, J. P. and J. Lalevée, *Photoinitiators for Polymer Synthesis: Scope, Reactivity and Efficiency*, First Edition, Wiley-VCH Verlag GmbH & Co. KGaA, Weinheim, pp. 73-87, 2012.

19. Fouassier, J. P. and J. Lalevée, *Photoinitiators for Polymer Synthesis: Scope, Reactivity and Efficiency*, First Edition, Wiley-VCH Verlag GmbH & Co. KGaA, Weinheim, pp. 127-186, 2012.

20. Decker, C., "Light-induced Crosslinking Polymerization", *Polymer International*, Vol. 51, pp. 1141-1150, 2002.

21. Green, W. A., *Industrial Photoinitiators: A Technical Guide*, CRC Press, Taylor & Francis Group, pp. 17-20, 2010.

22. Fouassier, J. P. and J. Lalevée, *Photoinitiators for Polymer Synthesis: Scope, Reactivity and Efficiency*, First Edition, Wiley-VCH Verlag GmbH & Co. KGaA, Weinheim, pp. 199-258, 2012.

23. Salamone, J., C., *Polymeric Materials Encyclopedia*, CRC Press Vol 10, pp. 7330-7332, 1996.

24. Liska R., "Photoinitiators with Functional Groups. VI. Chemically Bound Sensitizers", *Journal of Polymer Science*, Vol. 42, pp. 2285-2301, 2004.

25. Dietliker, K., S. Broillet, B. Hellrung, P. Rzadek, G. Rist, J. Wirz, D. Neshchadin and G. Gescheidt, "Photophysical Investigations on Photoinitiators with Covalently Linked Thioxanthone Sensitizer Moieties", *Helvetica Chimica Acta*, Vol. 89, pp. 2211-2225, 2006.

26. Wang, K., Y. Lu, P. Chen, J. Shi, H. Wang, Q. Yu, "Novel One-Component Polymeric Benzophenone Photoinitiator Containing Poly (Ethylene Glycol) as

Hydrogen Donor", *Materials Chemistry and Physics*, Vol. 143, pp. 1391-1395, 2014.

27. Yang, J., R. Tang, S. Sh, and J. Nie, "Synthesis and Characterization of Polymerizable One-Component Photoinitiator Based on Sesamol", *Photochemical and Photobiological Sciences*, Vol. 12, pp. 923-929, 2013.

28. Jiang, X., H. Xu and J. Yin, "Copolymeric Dendritic Macrophotoinitiators", *Polymer*, Vol. 46, pp. 11079-11084, 2005.

29. Angiolini, L., D. Caretti and E. Salatelli, "Synthesis and Photoinitiation Activity of Radical Polymeric Photoinitiators Bearing Side-Chain Camphorquinone Moieties", *Macromolecular Chemistry and Physics*, Vol. 201, pp. 2646-2653, 2000.

30. Angiolini, L., D. Caretti, C. Carlini, E. Corelli and E. Salatelli, "Polymeric Photoinitiators Having Benzoin Methylether Moieties Connected to the Main Chain Through the Benzyl Aromatic Ring and Their Activity for Ultraviolet-Curable Coatings", *Polymer*, Vol. 40, pp. 7197-7207, 1999.

31. Groot, H. D. J., K. Dillingham, H. Deuring, H. J. Haitjema, F. J. V. Beijama, K. Hodd and S. Norrby, "Hydrophilic Polymeric Acylphospine Oxide Photoinitiators/ Crosslinkers for in Vivo Blue-Light Photopolymerization", *Biomacromolecules*, Vol. 2, pp. 1271-1278, 2001.

32. Angiolini, L., D. Caretti, E. Corelli and C. Carlini, ''Copolymeric Systems with Pendant Thioxanthone and α-Morpholinoacetophenone Moieties as Photosensitizing and Photoinitiating Agents for UV-Curable Pigmented Coatings", *Journal of Applied Polymer Science*, Vol. 55, pp. 1477-1488, 1995.

33. Wang, H., J. Wei, X. Jiang and J. Yin, "Novel Chemical-Bonded Polymerizable Sulfur-Containing Photoinitiators Comprising the Structure of Planar *N*-phenylmaleimide and Benzophenone for Photopolymerization", *Polymer*, Vol. 47, pp. 4967-4975, 2006.

34. Nayak, B. R. and L. J. Mathias, "A Novel Photoinimer for the Polymerization of Acrylates and Methacrylates", *Journal of Polymer Science: Part A: Polymer Chemistry*, Vol. 43, pp. 5661-5670, 2005.

35. Karahan, O., D. Karaca Balta, N. Arsu and D. Avci, "Synthesis and Evaluations of Novel Photoinitiators with Side-Chain Benzophenone, Derived from Alkyl α-hyrdoxymethacrylates", *Journal of Photochemistry and Photobiology A: Chemistry*, Vol. 274, pp. 43-49, 2014.

36. Karaca Balta, D., O. Karahan, D. Avci and N. Arsu, "Synthesis, Photophysical and Photochemical Studies of Benzophenone Based Novel Monomeric and Polymeric Photoinitiators" *Progress in Organic Coatings*, Vol. 78, pp. 200-207, 2015.

37. Cesur, B., O. Karahan, S. Agopcan, T. N. Eren, N. Okte, D. Avci, "Difunctional Monomeric and Polymeric Photoinitiators: Synthesis and Photoinitiating Behaviours", *Progress in Organic Coatings*, Vol. 86, pp. 71-78, 2015.

38. Corrales, T., C. Peinado, F. Catalina, M. G. Neumann, N. S. Allen, A. M. Rufs and M. V. Encinas, "Photopolymerization of Methyl Methacrylate Initiated by Thioxanthone Derivatives: Photoinitiation Mechanism", *Polymer,* Vol. 41, pp. 9103-9109, 2000.

39. Corrales, T., F. Catalina, C. Peinado, N. S. Allen, "Free Radical Macrophotoinitiators: An Overview on Recent Advances", *Journal of Photochemistry and Photobiology A*, Vol. 159, pp. 103-114, 2003.

40. Allonas, X., J. P. Fouassier, L. Angiolini and D. Caretti, "Excited-State Properties of Camhorquinone Based Monomeric and Polymeric Photoinitiators", *Helvetica Chimica Acta.*, Vol. 84, pp. 2577-2588, 2001.

41. Wei, J. and F. Liu, "Novel Highly Efficient Macrophotoinitiator Comprising Benzophenone, Coinitiator Amine, and Thio Moieties for Photopolymerization", *Macromolecules*, Vol. 42, pp. 5486-5491, 2009.

42. Wang, J., J. Cheng, J. Liu, Y. Gao and F. Sun, "Self-floating Ability and Initiating Gradient Photopolymerization of Acrylamide Aqueous Solution of a Water-soluble Polysiloxane Benzophenone Photoinitiator", *Green Chemistry*, Vol. 15, pp. 2457-2465, 2013.

43. Jiang, X. and J. Yin, "Polymeric Photoinitiator Containing In-Chain Thioxanthone and Co-Initiator Amines", *Macromolecular Rapid Communications*, Vol. 25, pp. 748-752, 2004.

44. Temel, G., B. Aydogan, N. Arsu and Y. Yagci, "Synthesis and Characterization of One-Component Polymeric Photoinitiator by Simultaneous Double Click Reactions and Its Use in Photoinduced Free Radical Polymerization", *Macromolecules*, Vol. 42, pp. 6098-6106, 2009.

45. Wang, Y., X. Jiang and J. Yin, "Novel Polymeric Photoinitiators Comprising of Side-Chain Benzophenone and Coinitiator Amine: Photochemical and Photopolymerization Behaviors", *European Polymer Journal*, Vol. 45, pp. 437-447, 2009.

46. Chen, Y., J. Loccufier, L. Vanmaele and H. Frey, "Novel Multifunctional Hyperbranched Polymeric Photoinitiators with Built-in Amine Coinitiators for UV-Curing", *Journal of Materials Chemistry*, Vol. 17, pp. 3389-3392, 2007.

47. Si, Q., X. Fan, Y. Liu, J. Kong, S. Wang and W. Qiao, "Synthesis and Characterization of Hyperbranched-Poly(siloxysilane)-Based Polymeric Photoinitiators" *Journal of Polymer Scince, Part A: Polymer Chemistry*, Vol. *44*, pp. 3261-3270, 2006.

48. Xie, H., L. Hu, Y. Zhang and W. Shi, "Sulfur-Containing Hyperbranced Polymeric Photoinitiator End-Capped with Benzophenone and Tertiary Amine Moiteies Prepared via Simultaneous Double Thiol-Ene Click Reactions Used for UV Curing Coatings", *Progress in Organic Coatings*, Vol. 72, pp. 572-578, 2011.

49. Chen, Y., J. Loccufier, L. Vanmaele, E. Barriau and H. Frey, "Novel Multifunctional Polymeric Photoinitiators and Photo-Coinitiators Derived from

Hyperbranched Polyglycerol", *Macromolecular Chemistry and Phys*ics, Vol. 208, pp. 1694-1706, 2007.

50. Wen, Y., X. Jiang, R. Liu and J. Yin, "Amphipathic Hyperbranched Polymeric Thioxanthone Photoinitiators (AHPTXs): Synthesis, Characterization and Photoinitiated Polymerization", *Polymer*, Vol. 50, pp. 3917-3923, 2009.

51. Gacal, B., H. Akat, D. K. Balta, N. Arsu and Y. Yagci, "Synthesis and Characterization of Polymeric Thioxanthone Photoinitiators via Double Click Reactions" *Macromolecules,* Vol. *41,* pp. 2401-2405, 2008.

52. Akat, H., B. Gacal, D. K. Balta, N. Arsu and Y. Yagci, "Poly(ethyleneglycol)-Thioxanthone Prepared by Diels-Alder Click Chemistry as One-Component Polymeric Photoinitiator for Aqeous Free-Radical Polymerization", *Journal of Polymer Science., Part A: Polymer Chemistry,* Vol. 48, pp. 2109-2114, 2010.

53. Jiang, X., J. Luo and J. Yin, "A Novel Amphipathic Polymeric Thioxanthone Photoinitiator" *Polymer,* Vol. 50, pp. 37-41, 2009.

54. Kork, S., G. Yilmaz and Y. Yagci, "Poly(vinylalcohol)-Thioxanthone as One-Component Type II Photoinitiator for Free Radical Polymerization in Organic and Aqeous Media" *Macromolecular Rapid Communications*, Vol. 36, pp. 923-928, 2015.

55. Jiang, X. And J. Yin, "Study of Macrophotoinitiator Containing In-Chain Thioxanthone and Coinitiator Amines", *Polymer,* Vol. 45, pp. 5057-5063, 2004.

56. Corrales, T., F. Catalina, N. S. Allen and C. Peinado, *Journal of Photochemistry & Photobioogy, A,* Vol. 169, pp. 95-100, 2005.

57. Jiang, X. and J. Yin, "Dendritic Macrophotoinitiator Containing Thioxanthone and Coinitiator Amine", *Macromolecules,* Vol. 37, pp. 7850-7853, 2004.

58. Mathias, L. J., R. M. Warren and S. Huang, "*tert*-Butyl α-(hydroxymethyl)acrylate and Its Ether Dimer: Multifunctional Monomers Giving Polymers with Easily Cleaved Ester Groups", *Macromolecules*, Vol. 24, pp. 2036-2042, 1991.

59. Warren, S. C. and L. J. Mathias, "Synthesis and Polymerization of Ethyl α-Chloromethylacrylate and Related Derivatives", *Journal of Polymer Science: Part A: Polymer Chemistry*, Vol. 28, pp. 1637–1648, 1990.

60. Eren, T. N., *Photophysical and Photochemical Studies of Novel Thioxanthone Functionalized Methacrylates*, M.S. Thesis, Boğaziçi University, 2015.